Semi-Crystalline Polymer Morphologies and their Hierarchical Morphologies

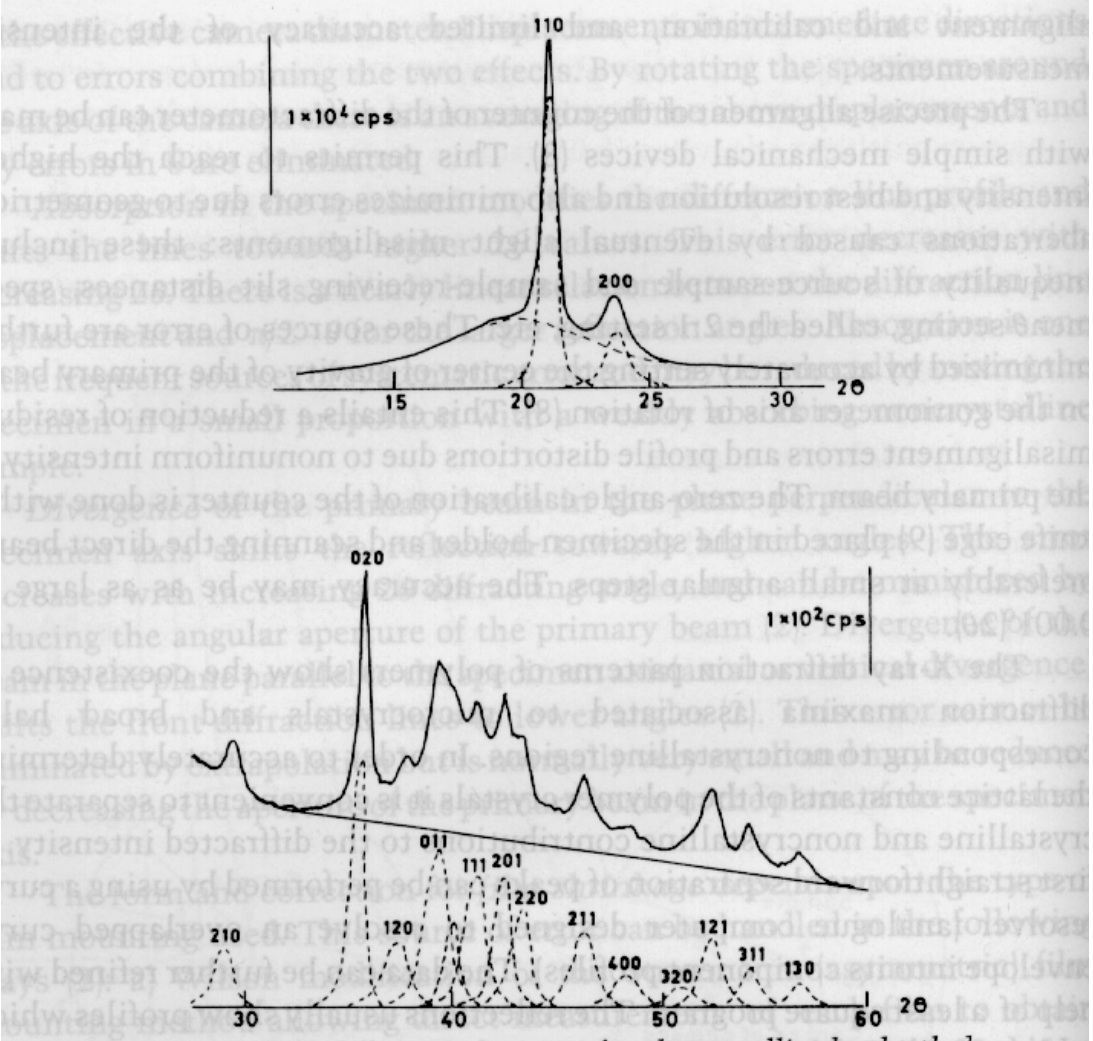

Fig. 3.3. Typical X-ray diffraction pattern of melt crystallized polyethylene illustrating the separation of crystalline and non crystalline maxima (Martinez Salazar (11)).

Semi-Crystalline Polymer Morphologies and their Hierarchical Morphologies

Semi-Crystalline
Helical Structure
Chain Folding
Semi-Crystalline Fibrillar Growth
Spherulitic, shish-kabob, epitaxial surface nucleation,
Crystalline Orientation
Lamellar Orientation
Macroscopic Orientation

Semi-Crystalline Polymer Morphologies and their Hierarchical Morphologies

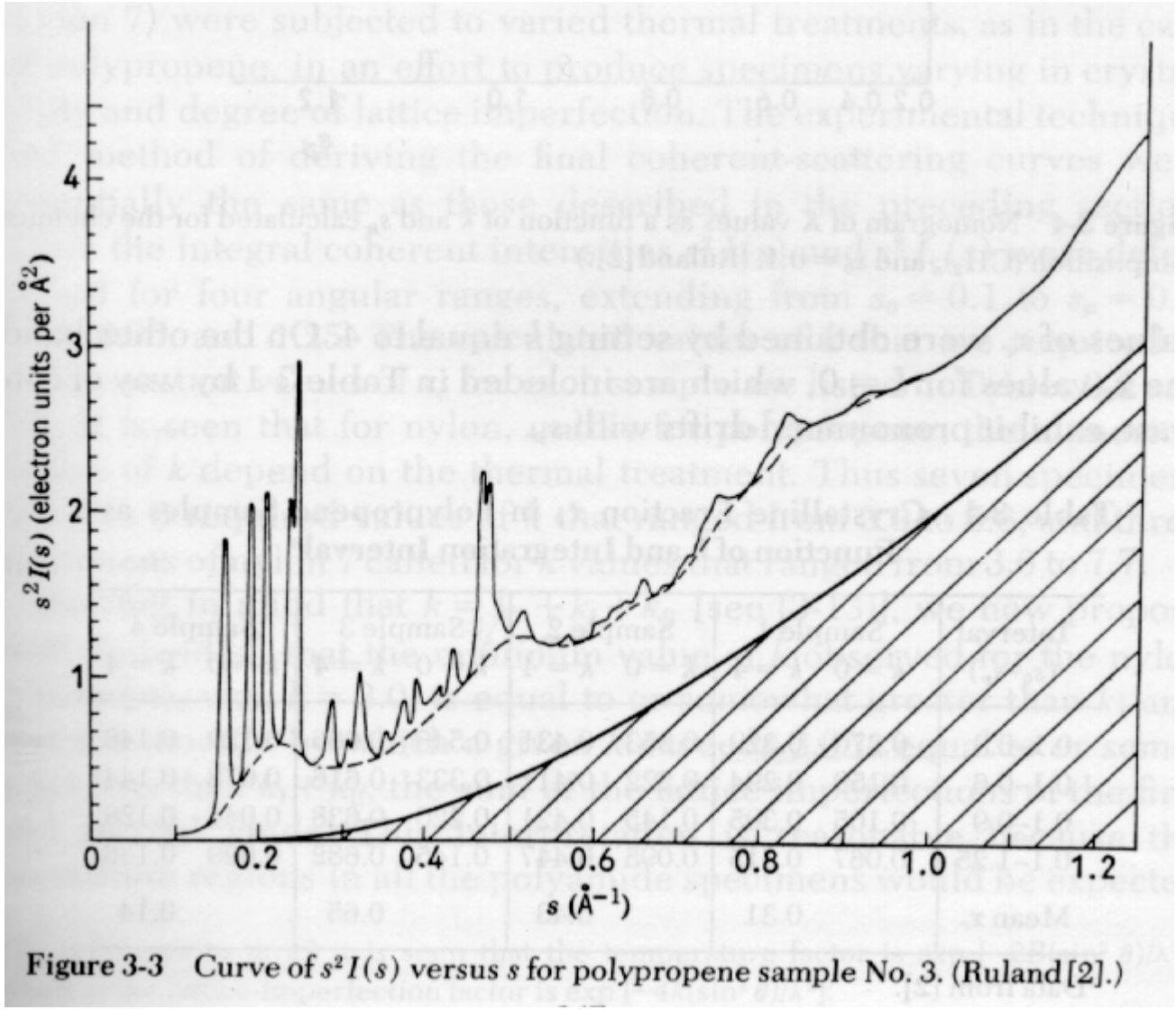

Figure 3-3 Curve of $s^2 I(s)$ versus s for polypropene sample No. 3. (Ruland [2].)

Semi-Crystalline Polymer Morphologies and their Hierarchical Morphologies

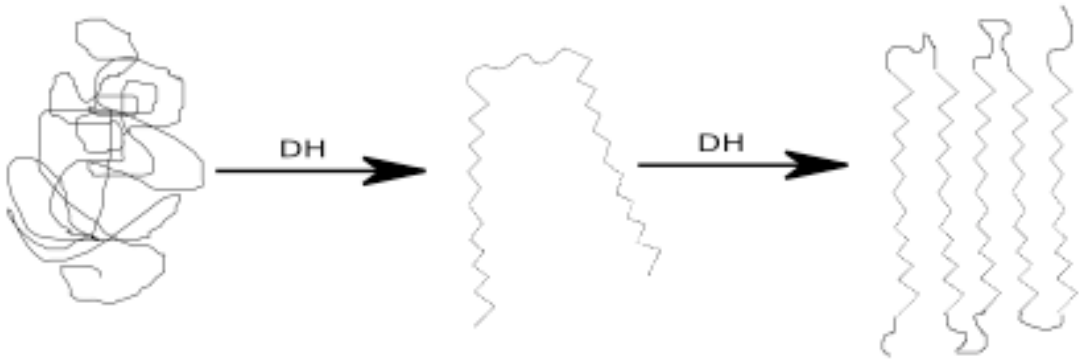

Semi-Crystalline Polymer Morphologies and their Hierarchical Morphologies

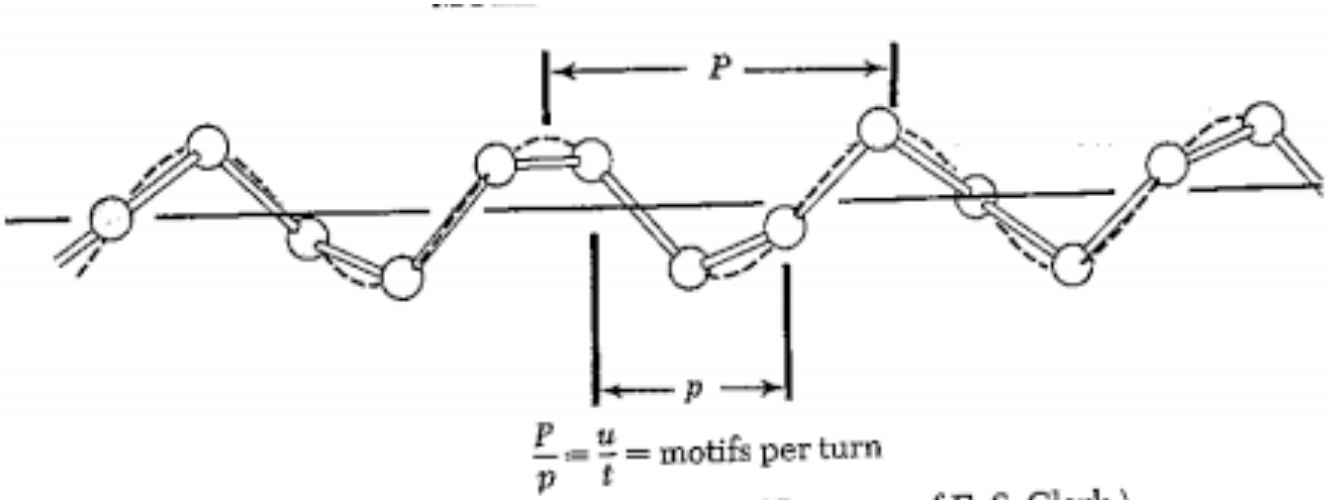

Figure 6-1 Helical nomenclature. (Courtesy of E. S. Clark.)

p = Z-axis projection of the distance between consecutive equivalent points on the helix;

u = number of points, or motifs, on the helix corresponding to the period c (an integer);

t = number of turns of the helix in the identity period c (an integer);

$\Delta\Phi$ = projection on a plane perpendicular to Z of the central angle defined by two successive equivalent points on the helix;

γ = a positive integer > 0;

ϵ = a positive integer ≥ 0.

Semi-Crystalline Polymer Morphologies and their Hierarchical Morphologies

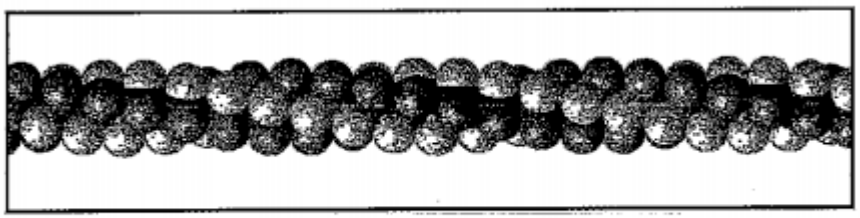

Fig. 2.3. PTFE in the crystalline state. The conformation corresponds to a 13/6-helix

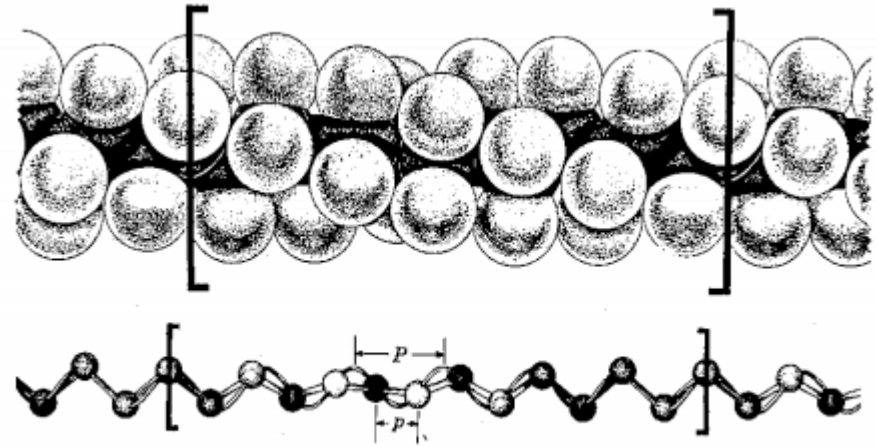

Figure 6-9 Molecular conformation of polytetrafluoroethylene: top—repeat unit of one molecule; bottom—carbon skeleton showing 13/6 helix. (Clark and Muus [27].)

Semi-Crystalline Polymer Morphologies and their Hierarchical Morphologies

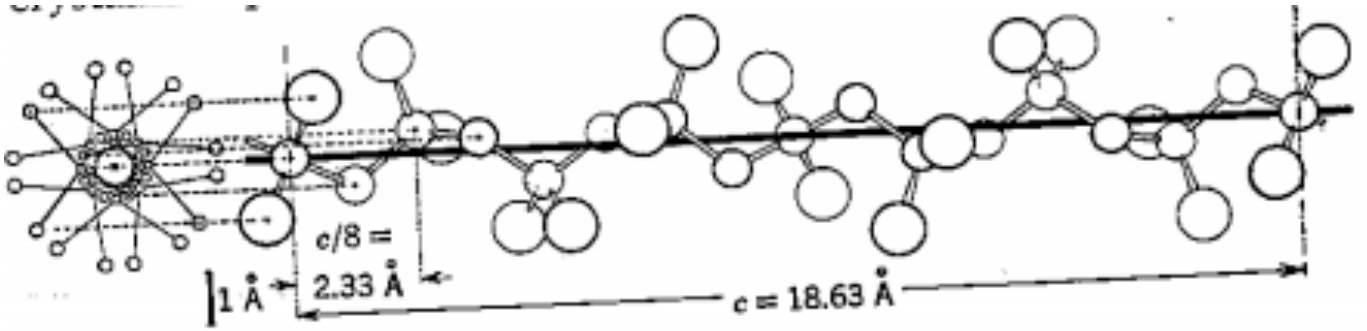

Figure 6-8 The 8/5 helix of the polyisobutene molecule. Small circles = CH_2; large circles = CH_3. (Liquori [25].)

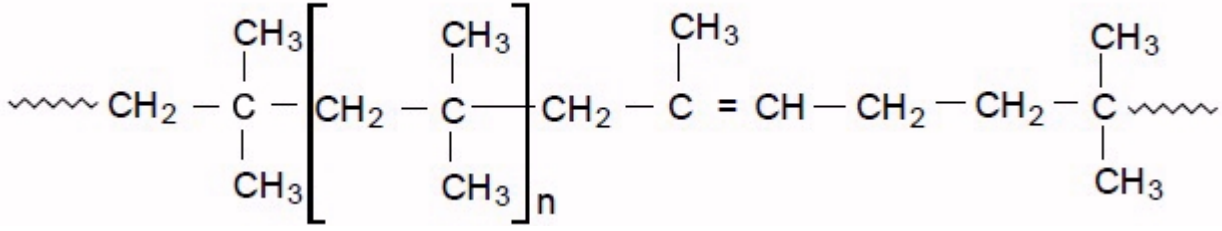

Semi-Crystalline Polymer Morphologies and their Hierarchical Morphologies

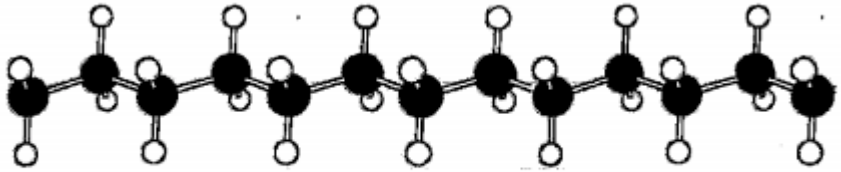

Fig. 2.1. The steric structure of PE. Rotations about the C–C bonds result in a change in the conformation

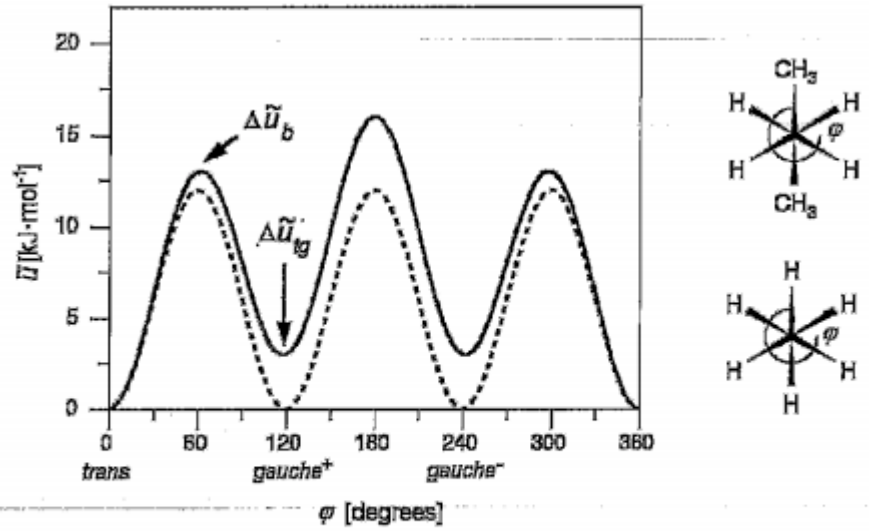

Fig. 2.2. Potential energies associated with the rotation of the central C–C bond for ethane (*broken line*) and butane (*continuous line*). The *sketches* show the two molecules in views along the C–C bond

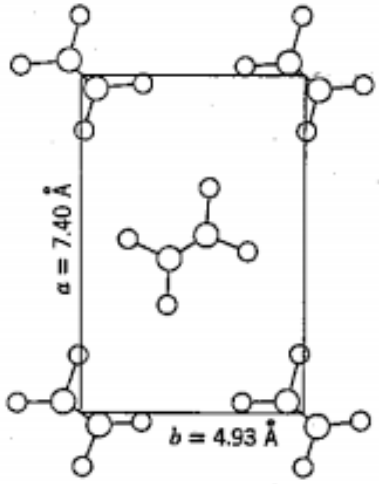

Figure 6-40 Arrangement of the molecules of polyethylene in the *c*-projection. (Courtesy of E. S. Clark.)

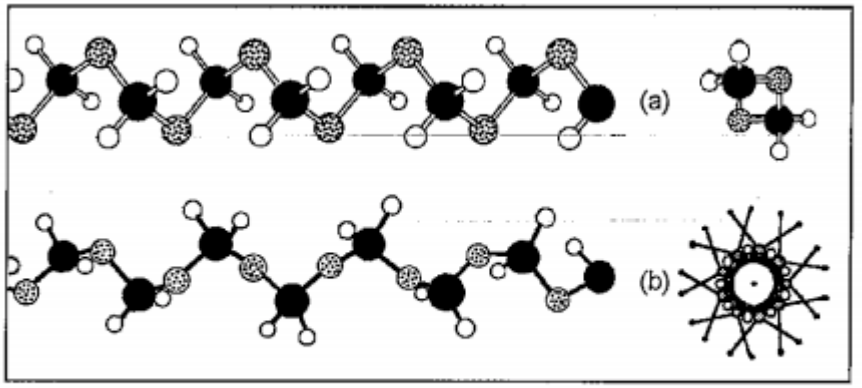

Fig. 2.4. Two different helices formed by POM: 2/1-helix (a) and 9/5-helix (b). Side views (*left*) and views along the helix axis (*right*)

Semi-Crystalline Polymer Morphologies and their Hierarchical Morphologies

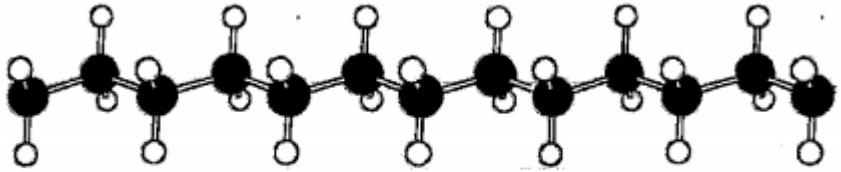

Fig. 2.1. The steric structure of PE. Rotations about the C–C bonds result in a change in the conformation

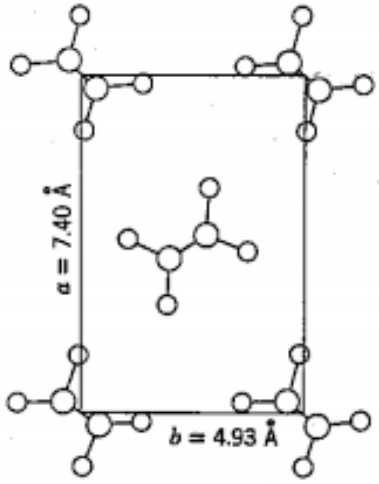

Figure 6-40 Arrangement of the molecules of polyethylene in the *c*-projection. (Courtesy of E. S. Clark.)

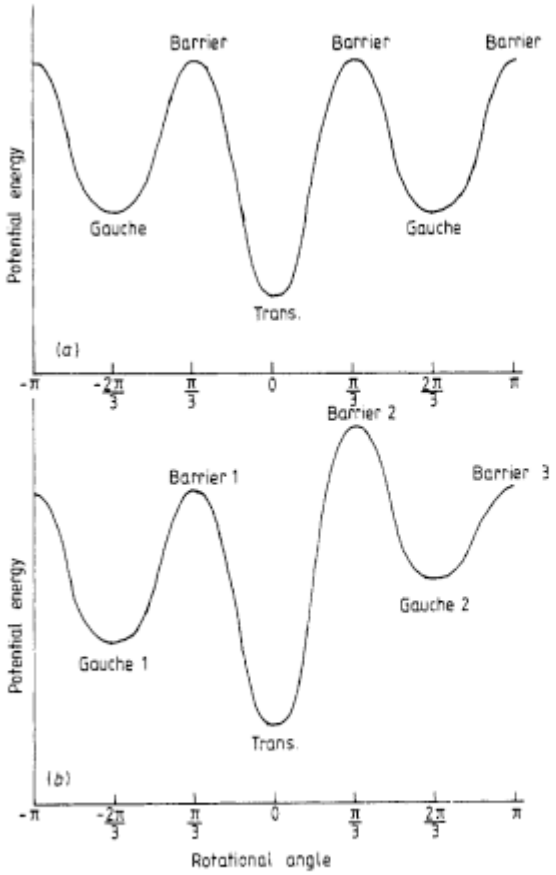

Figure 1. Schematic potential energy diagrams of rotation for (*a*) polyethylene and (*b*) a vinyl polymer.

Paul Phillips
1990 Review

Semi-Crystalline Polymer Morphologies and their Hierarchical Morphologies

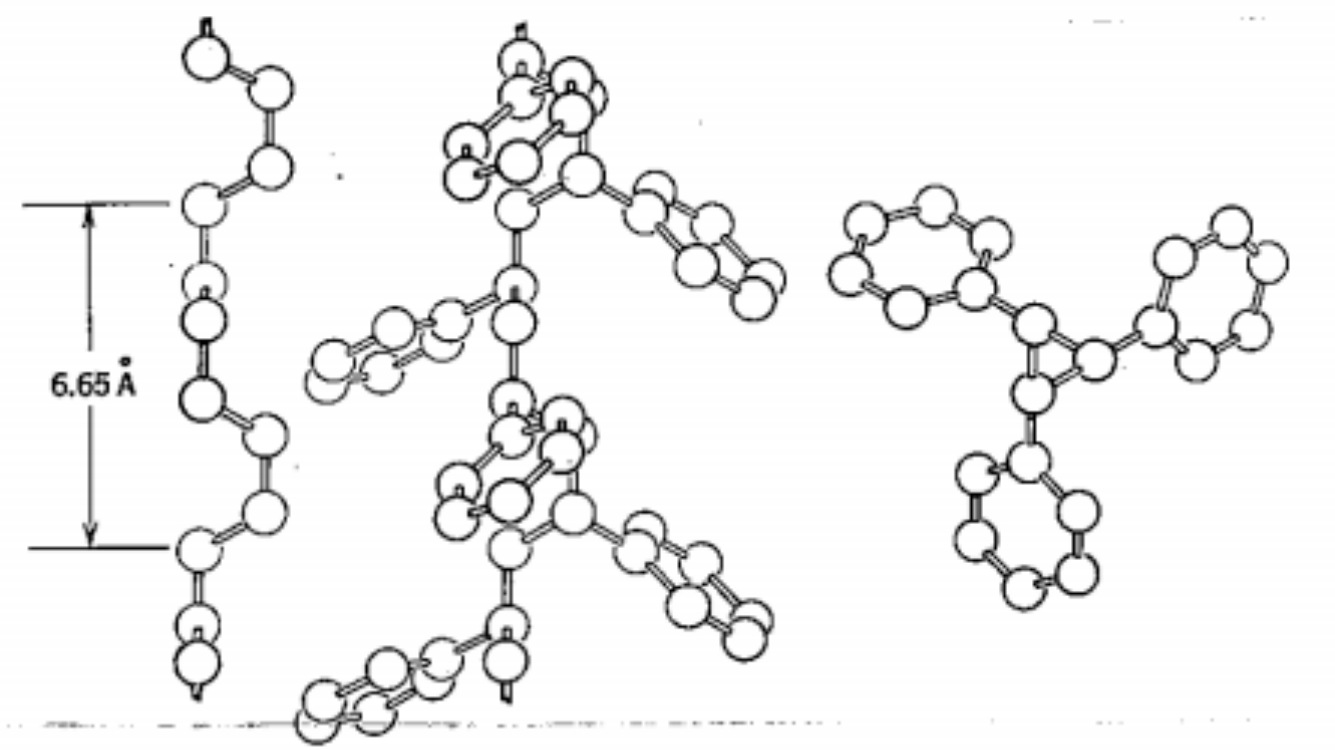

Figure 6-7 Left: the chain $(TG)_5$. Center and right: side and end views of the isotactic polystyrene molecule. (Bunn and Howells [17].)

P J Phillips

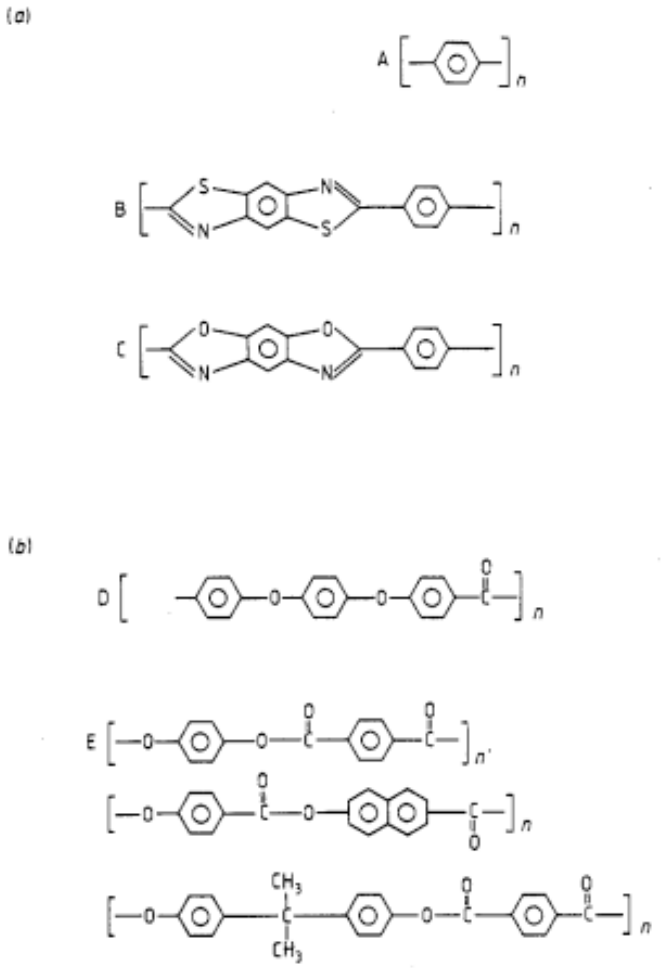

Figure 2. Examples of (*a*) rigid and (*b*) semi-rigid polymer molecules. A, poly(p-phenylene); B, poly(p-phenylene benzobisthiazole); C, poly(p-phenylene benzimidazole); D, poly(ether ether ketone); E, some thermotropic copolyesters.

Kevlar

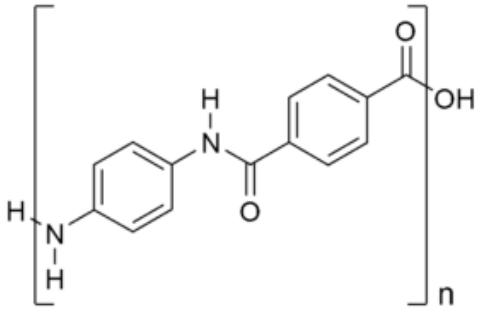

Rigid, semi-Rigid, Flexible Polymer Chains

On melting the entropy gain is small because the crystallizing units are chemically bound. The random coil state is seen classically as the highest entropy state. For rigid polymers the ground state may be a lower entropy state.

Polythiophene

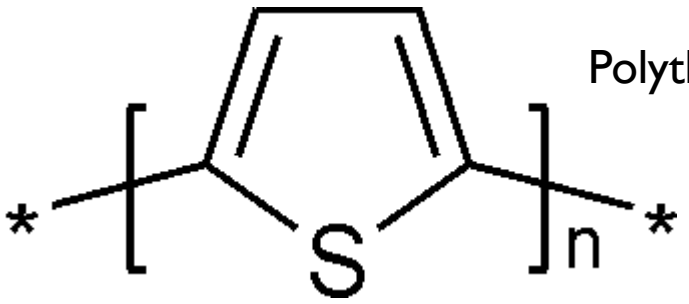

Paul Phillips
1990 Review

Semi-Crystalline Polymer Morphologies and their Hierarchical Morphologies

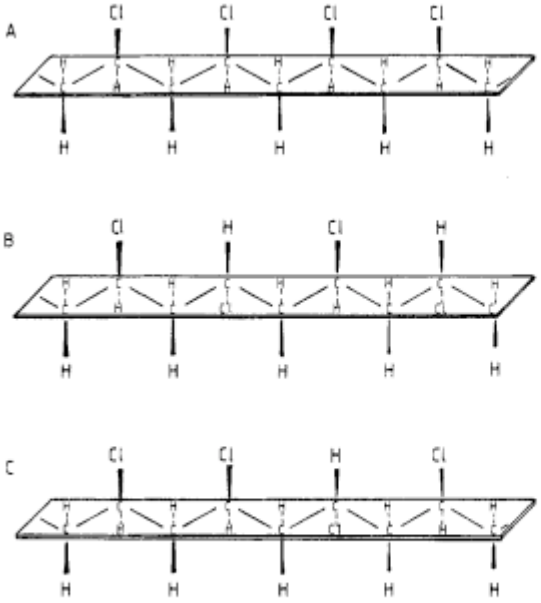

Figure 3. Major tacticity types in poly(vinyl chloride). A, isotactic; B, syndiotactic; C, atactic.

Tacticity

Tacticity governs the helical structure

Paul Phillips
1990 Review

Semi-Crystalline Polymer Morphologies and their Hierarchical Morphologies

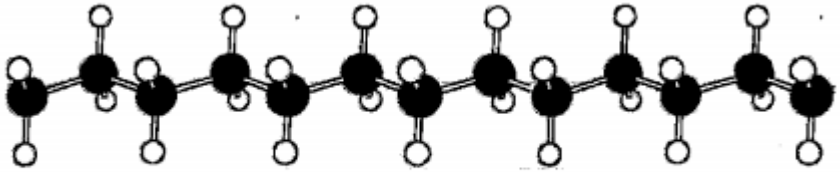

Fig. 2.1. The steric structure of PE. Rotations about the C–C bonds result in a change in the conformation

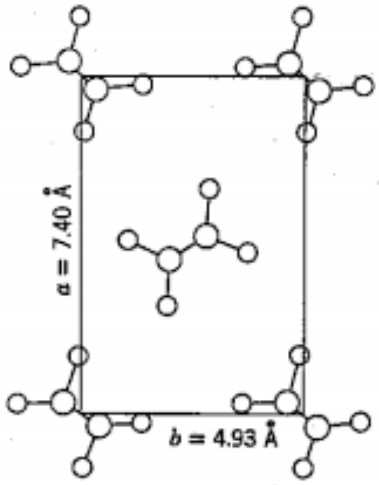

Figure 6-40 Arrangement of the molecules of polyethylene in the *c*-projection. (Courtesy of E. S. Clark.)

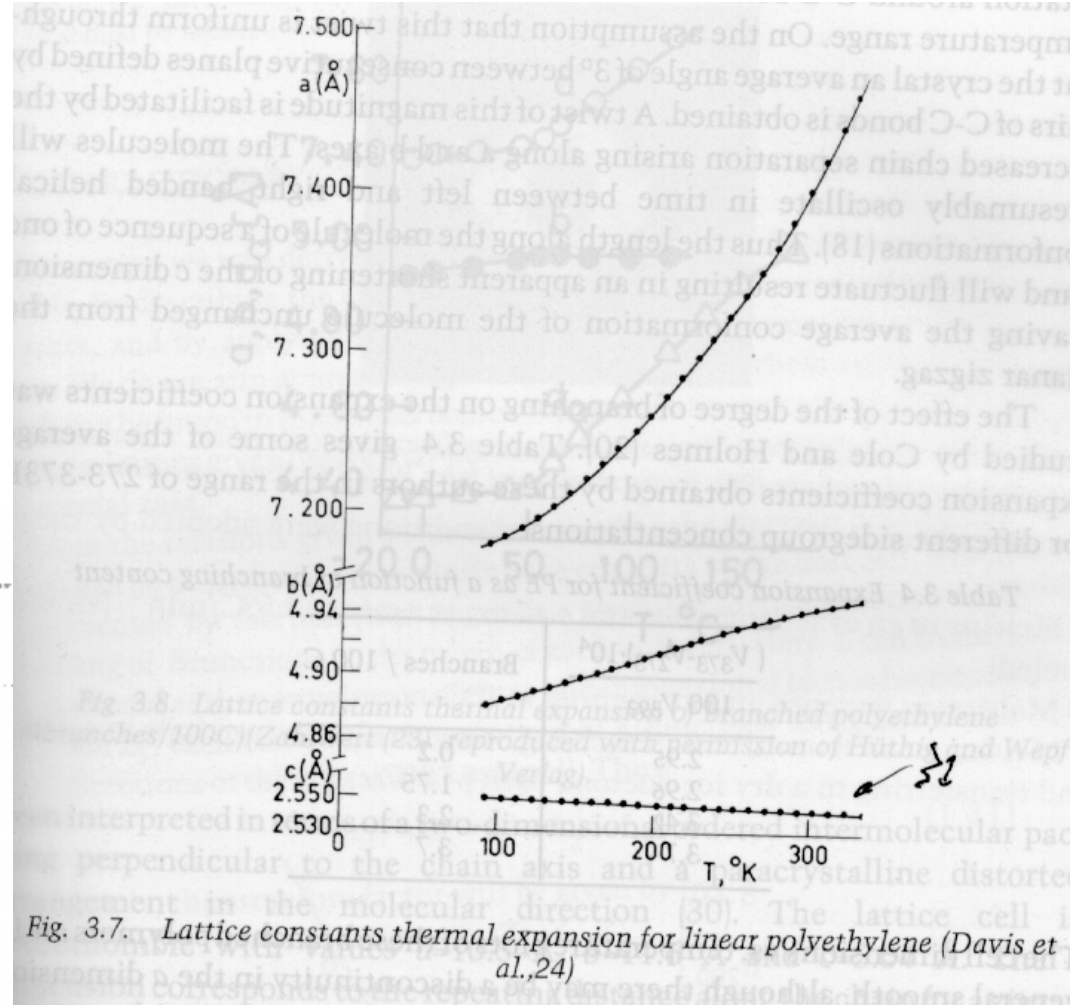

Fig. 3.7. Lattice constants thermal expansion for linear polyethylene (Davis et al.,24)

Semi-Crystalline Polymer Morphologies and their Hierarchical Morphologies

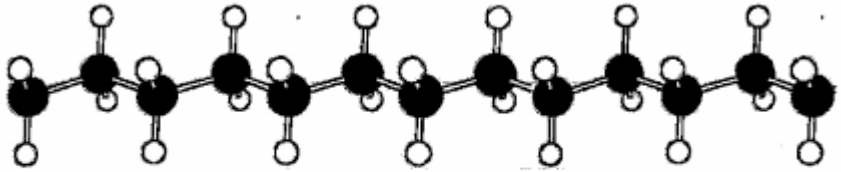

Fig. 2.1. The steric structure of PE. Rotations about the C–C bonds result in a change in the conformation

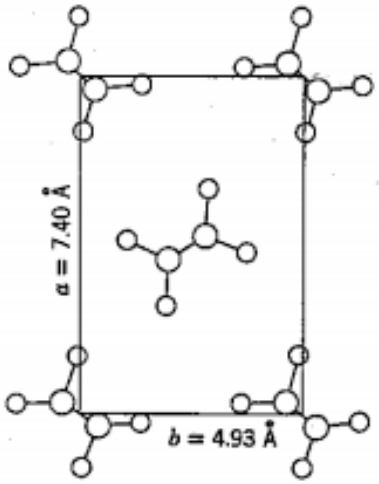

Figure 6-40 Arrangement of the molecules of polyethylene in the *c*-projection. (Courtesy of E. S. Clark.)

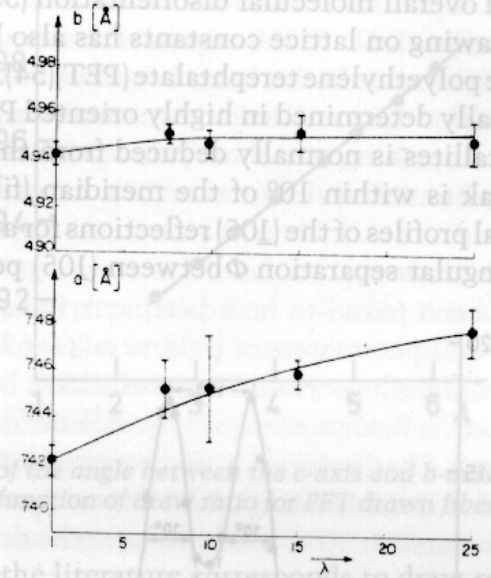

Fig. 3.18. a- and b-lattice constants of PE as a function of draw ratio (Glenz et al.(47);reproduced with permission by John Wiley & Sons, publishers.).

Semi-Crystalline Polymer Morphologies and their Hierarchical Morphologies

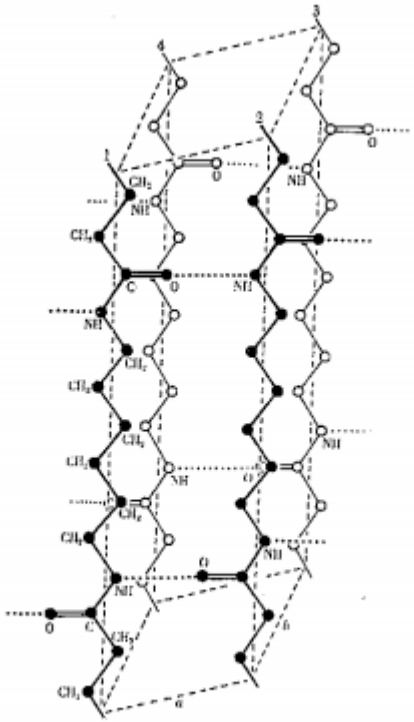

Figure 1-5 Arrangement of molecular chains in nylon 66, poly(hexamethylene adipamide). (Bunn and Garner [6].)

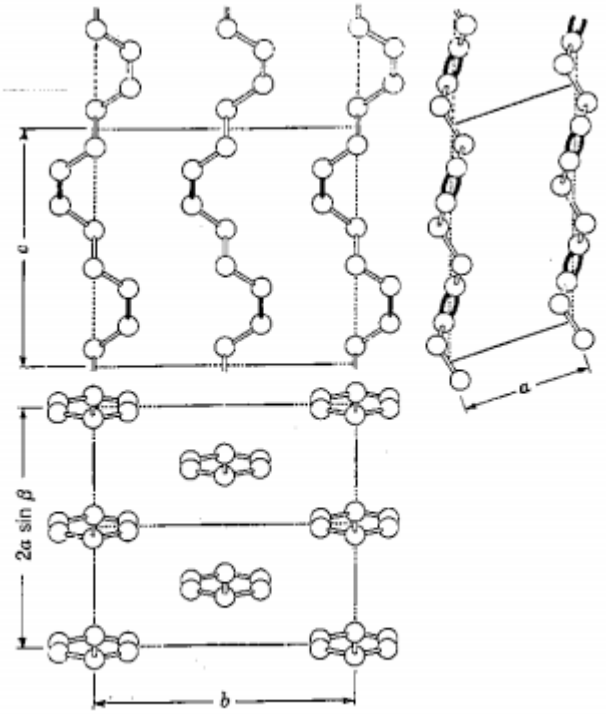

Figure 1-6 Structure of *cis* 1,4-polybutadiene as seen in three projections. Monoclinic unit cell with $a = 4.60$, $b = 9.50$, $c = 8.60$ Å; $\beta = 109°$. (Natta and Corradini [7].)

Semi-Crystalline Polymer Morphologies and their Hierarchical Morphologies

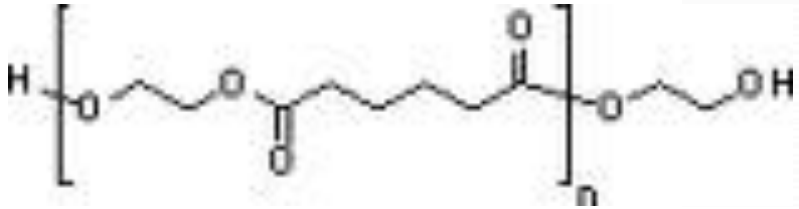

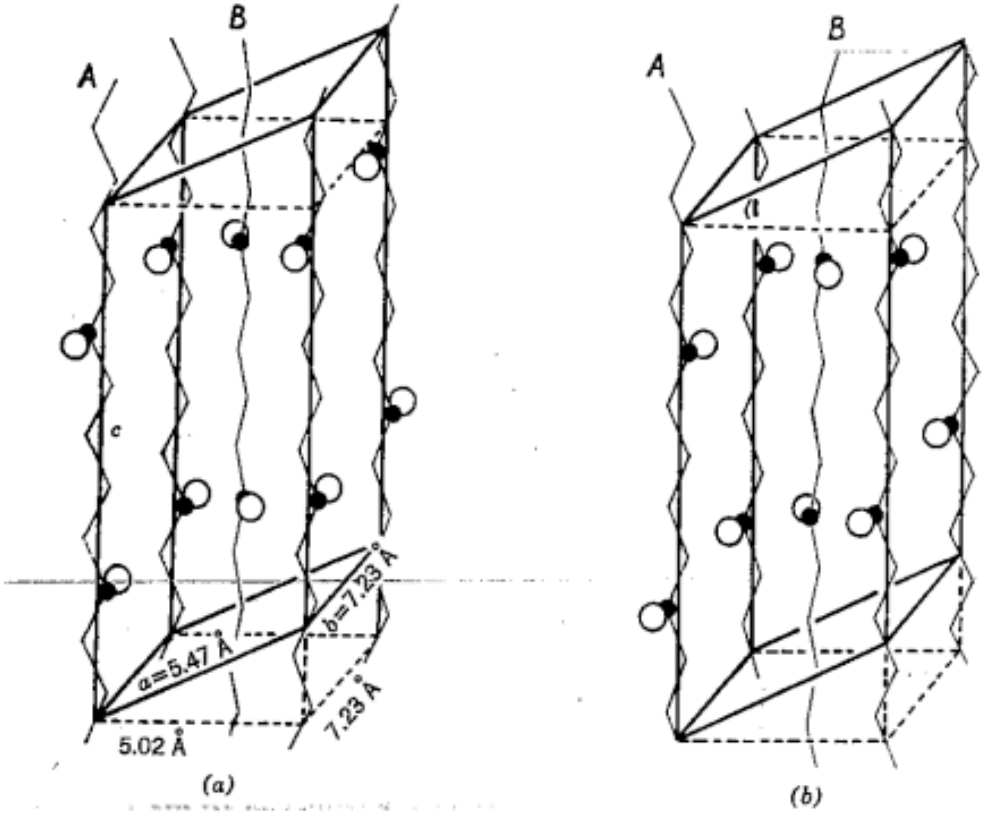

Figure 6-35 Unit cell of poly(ethylene adipate) and the two possible orientations of the molecular chain. (Turner-Jones and Bunn [84].)

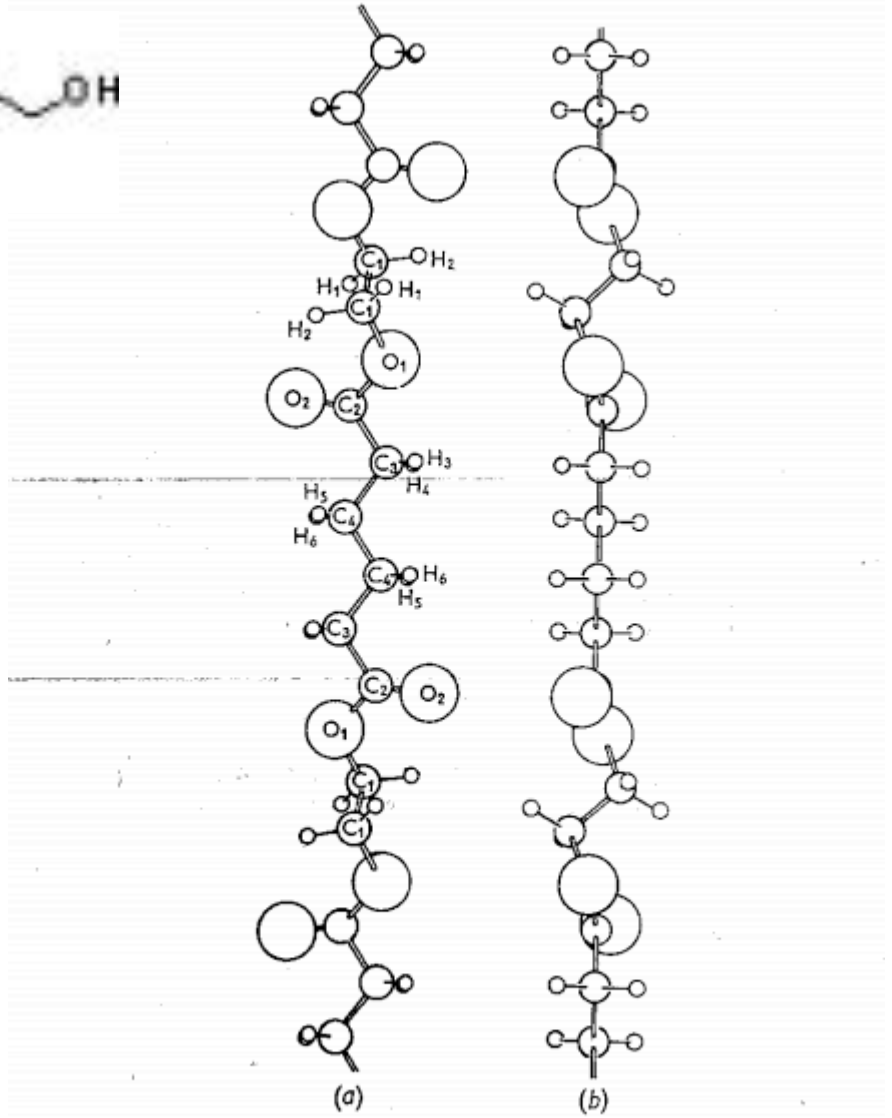

Figure 6-37 Chain configuration of poly(ethylene adipate) viewed (*a*) perpendicular and (*b*) parallel to the plane of the adipate chain. (Turner-Jones and Bunn [84].)

Semi-Crystalline Polymer Morphologies and their Hierarchical Morphologies

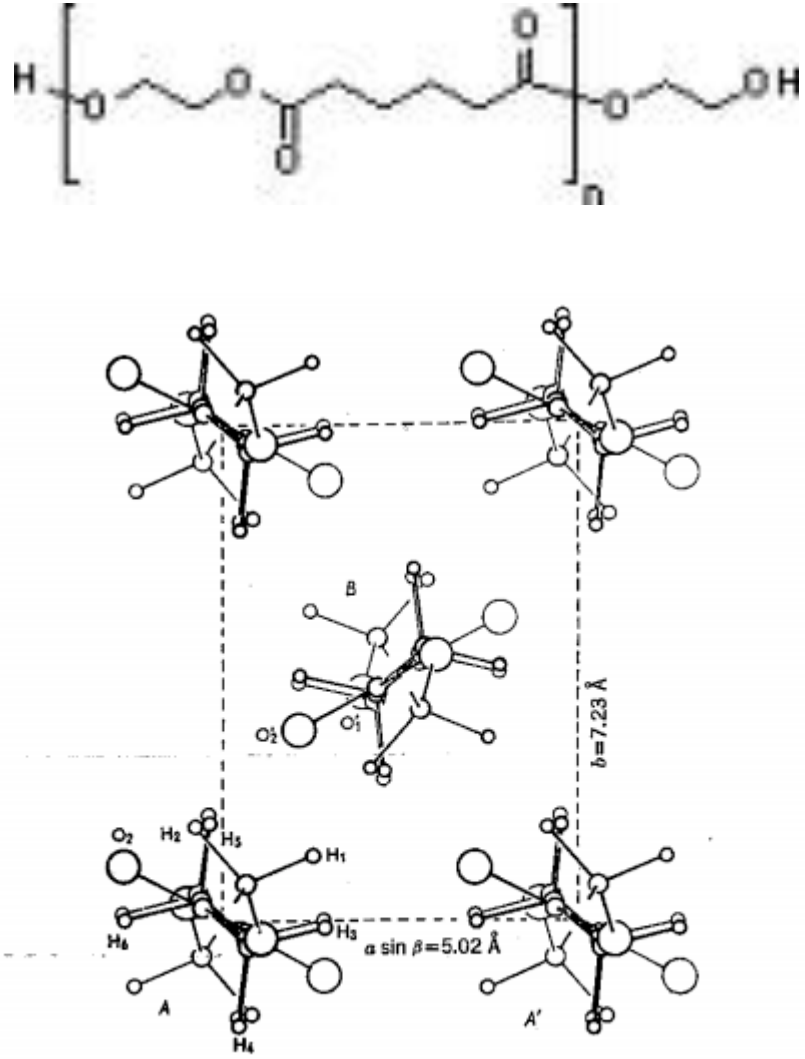

Figure 6-38 Arrangement of the molecules in the *c*-projection. (Turner-Jones and Bunn [84].)

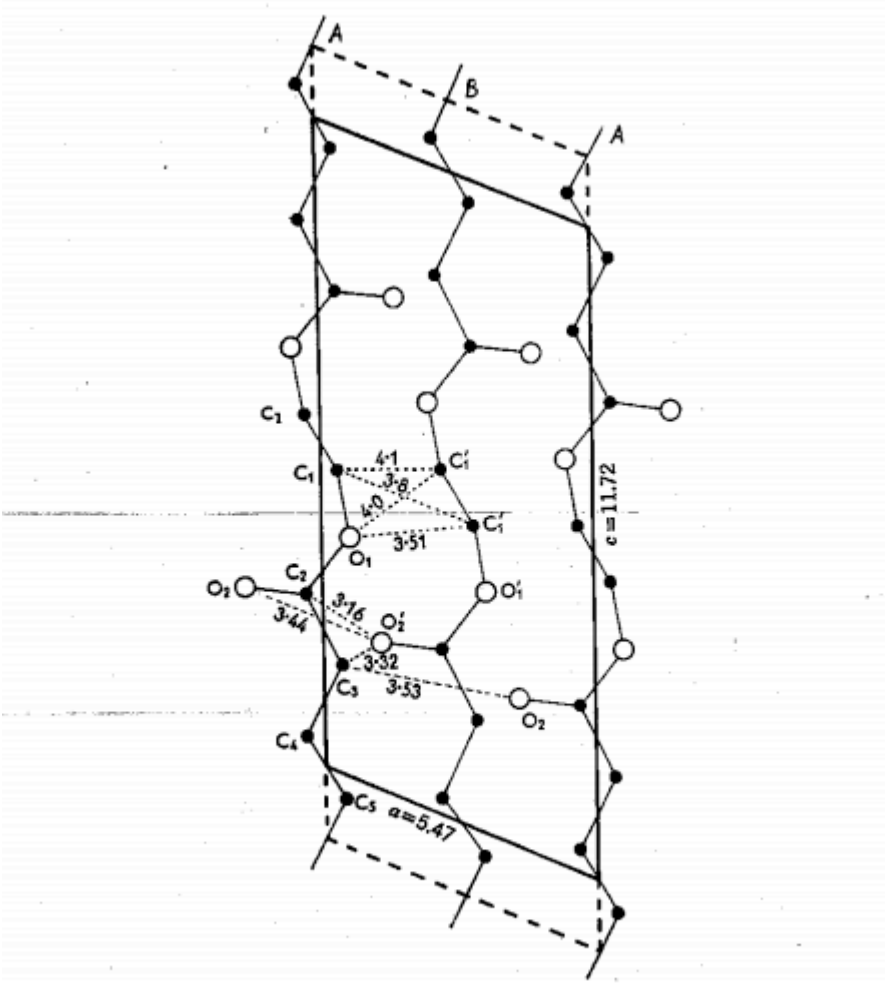

Figure 6-39 Arrangement of the molecules in the *b*-projection. All distances are in angstroms. (Turner-Jones and Bunn [84].)

Chain Folding and Crystallization

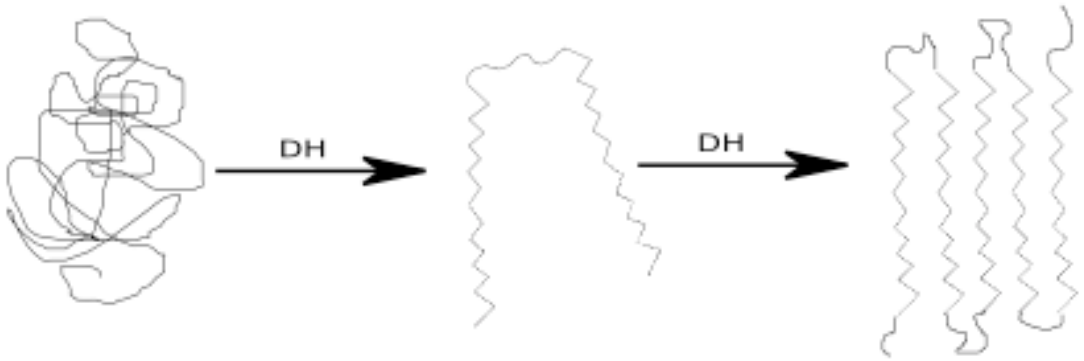

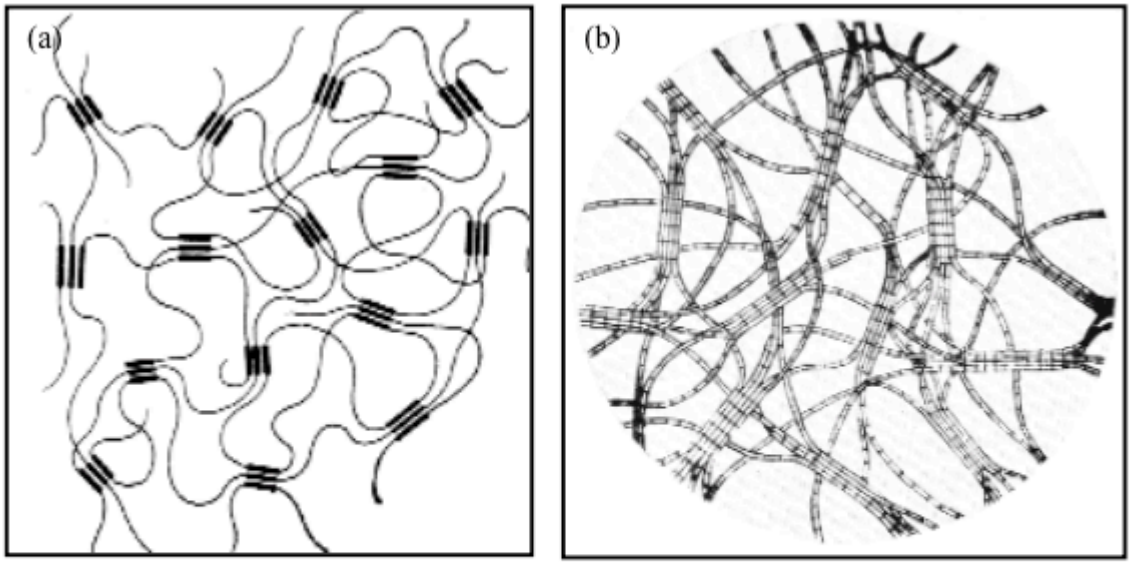

Figure 2.5 Fringed micelle model (a) Model of crystallization as might be visualized in a thermoreversible gel (Keller et al[10].) (b) Hermann and Gerngross model[15] for a semicrystalline polymer. Similar schematics illustrate the general molecular picture in fringed micellar crystallization.

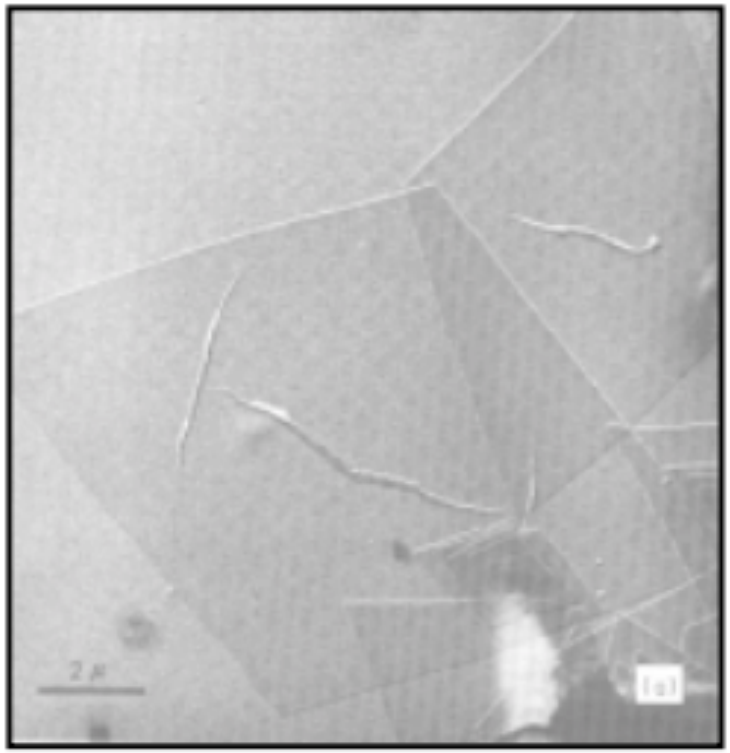

Figure 2.6 Single crystals of Polyethylene after evaporation of tetrachloroethylene solvent. Pleats form due to crystal collapse. Micrograph is taken from 'Polymer Single Crystals' by P.H. Geil[19].

Semi-Crystalline Polymer Morphologies and their Hierarchical Morphologies

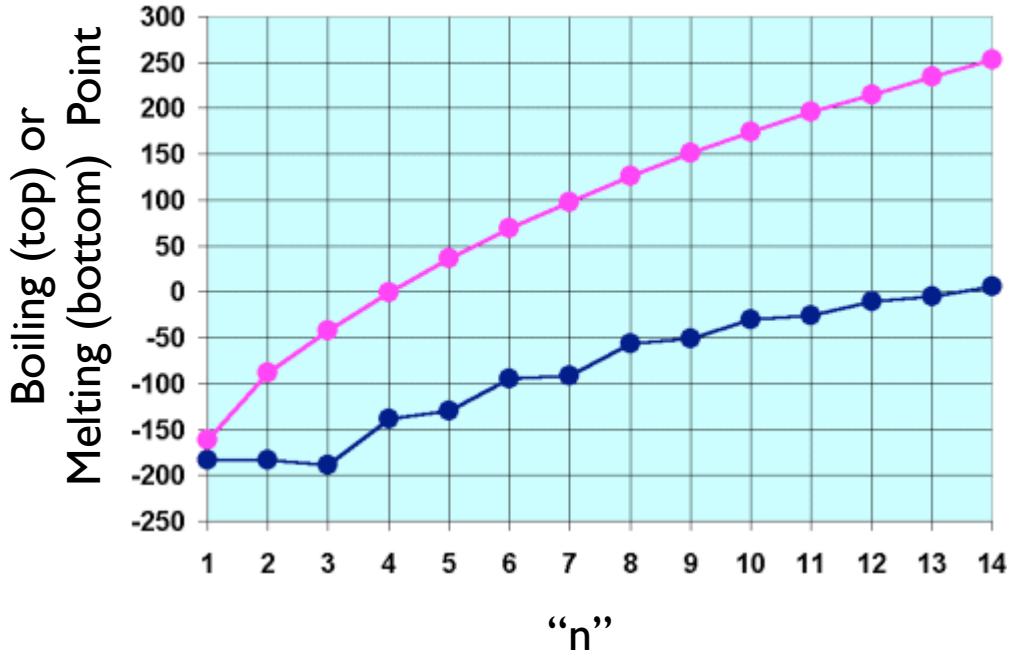

n-alkane boiling and melting points

Semi-Crystalline Polymer Morphologies and their Hierarchical Morphologies

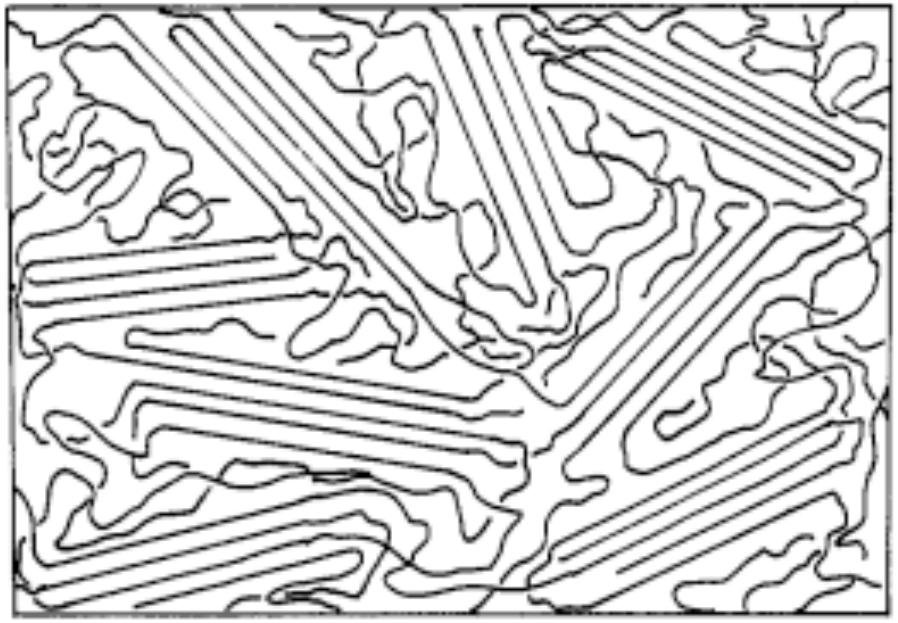

Figure 4. Schematic diagram of the fringed micelle model of polymer crystals.

"Crystals act like crosslinks in rubber" P. Phillips 1990

Semi-Crystalline Polymer Morphologies and their Hierarchical Morphologies

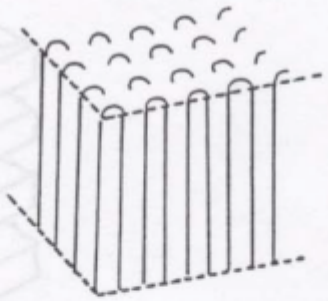

Fig. 16. The adjacent re-entry model of molecular re-entry.

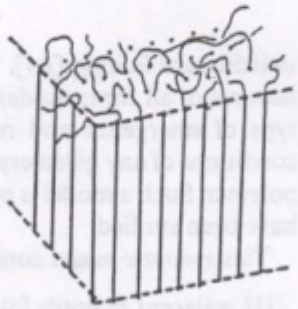

Fig. 17. The switchboard, or non-adjacent re-entry, model of molecular re-entry.

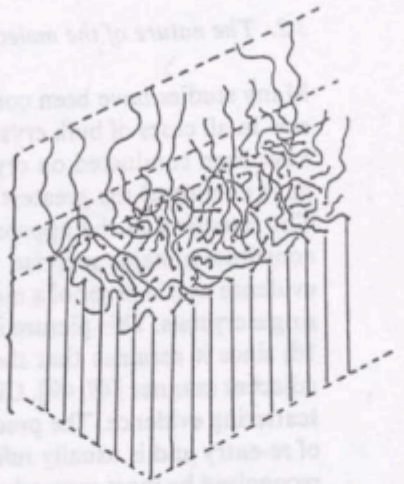

Fig. 18. The interzonal model of molecular re-entry.

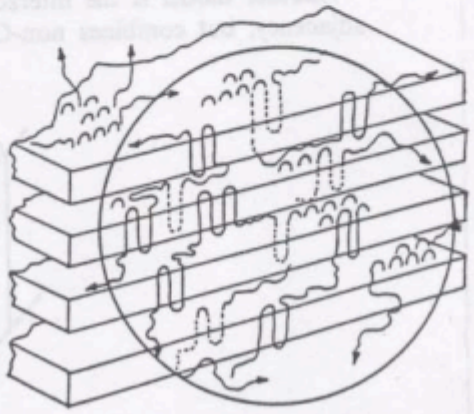

Fig. 19. The synoptic, or comprehensive, model of molecular re-entry. The circle represents the radius of gyration of a typical high-molecular-weight polymer.

Semi-Crystalline Polymer Morphologies and their Hierarchical Morphologies

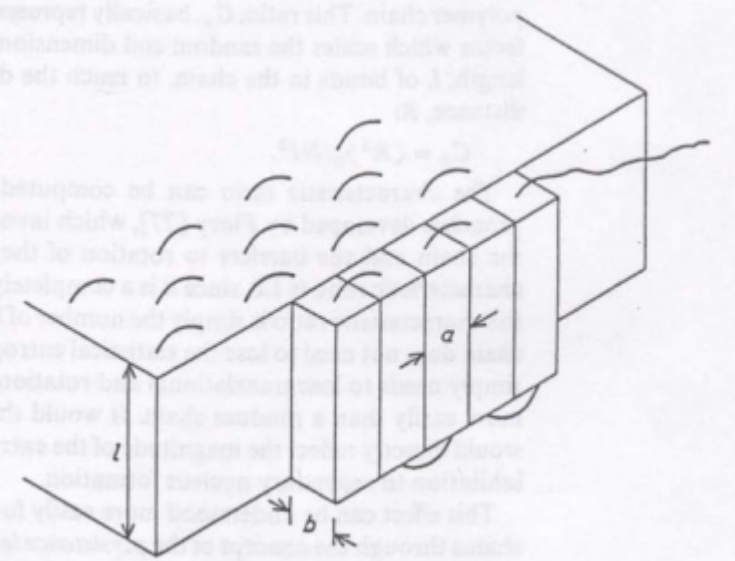

Fig. 20. Stem deposition model of secondary necleation.

(1) Random reentry or "Switchboard" folded model.

This model was first proposed by Flory[17,29,30,31] and consists of chains randomly folding back into the same lamella or even participating in adjoining lamellae. The upper and lower surfaces consist of loops of varying sizes and the amount of adjacent reentry is *small* and *not a necessity*[17,29,30,31]. The upper and lower surfaces may consist of transitional regions that constitute a diffuse phase boundary – their density being intermediate between the crystal and purely amorphous regions.

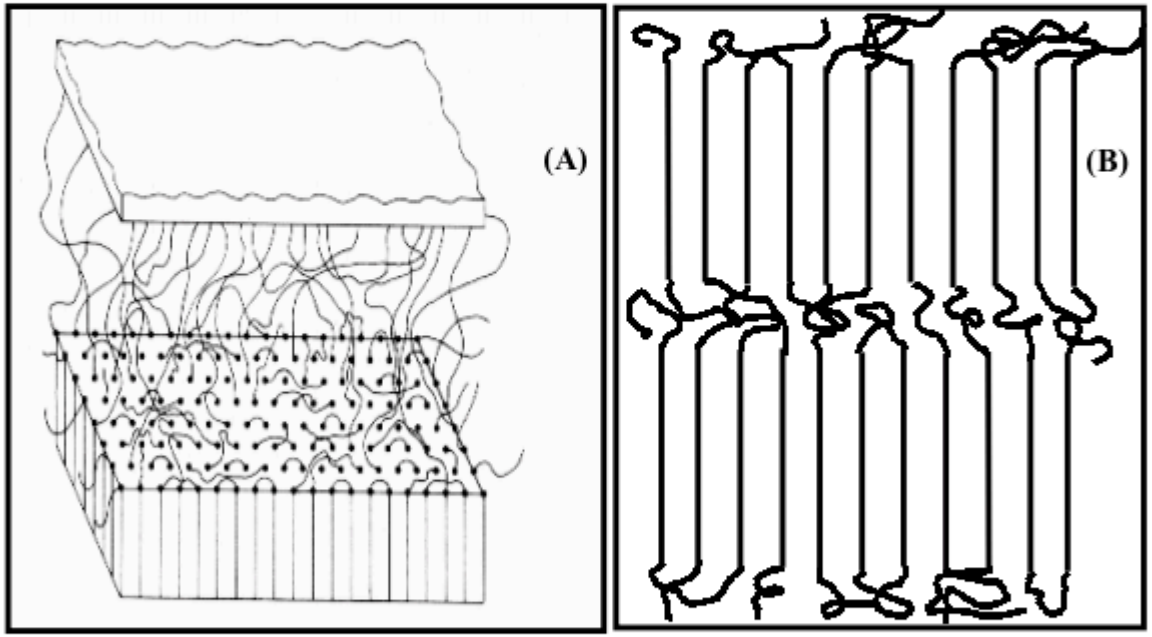

Figure 2.7 (A) Schematic of a Switchboard model, showing the surface of a lamella, interlamellar region and tie chains between the lamella. (From Mandelkern[30]) (B) originally proposed model for melt crystallization in polymers[17].

(2) **Adjacent reentry chain-folded models (regular folding)**

(i) *Smooth surface model*[32,33]*:*

This model is characterized by sharp phase boundary between the crystal and the amorphous phase. The mode of reentry of the chains is the adjacent neighbor with only a few exceptions due to multiple nucleation and chain-end defects. This is a very idealized visualization of the chain folding process.

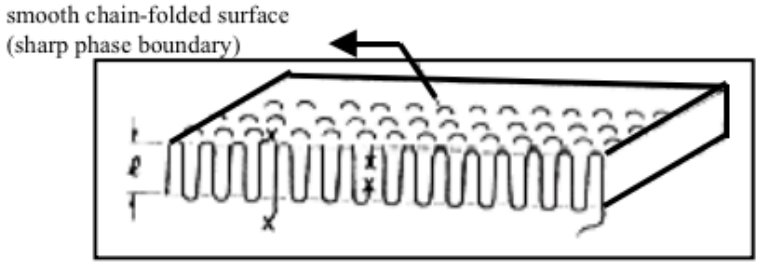

(ii) *Rough surface model*[33]*:*

The reentry of the chain is still in the nearest growth plane, though large variations in the fold length may exist on a local scale. Multiple nucleation and chain-end defects will further contribute to a rough surface. The overall phase boundary is no longer sharp, though local regions may still exhibit such character.

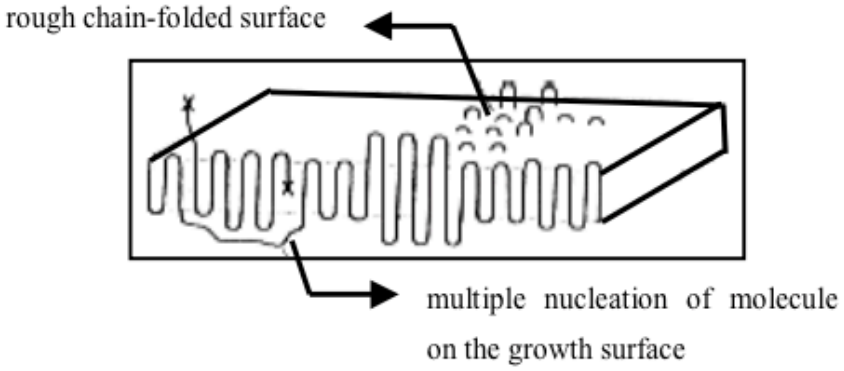

(3) *"Erstarrungsmodell"* (solidification model)[34,35]

This model was put forward by Fischer & coworkers to explain the constancy of the radius of gyration r_g in the crystalline state (with respect to r_g in the amorphous state), as detected by small angle neutron scattering (SANS)[36]. The model is similar in conception to the "fringed micellar" morphology and is visualized in terms of alignment of chains without a long-range diffusion process to give rise to a lamellar morphology. The chain sequences in proper conformations (indicated by thicker lines in the diagram) are incorporated into the crystal without significant reorganization of the chain conformation.

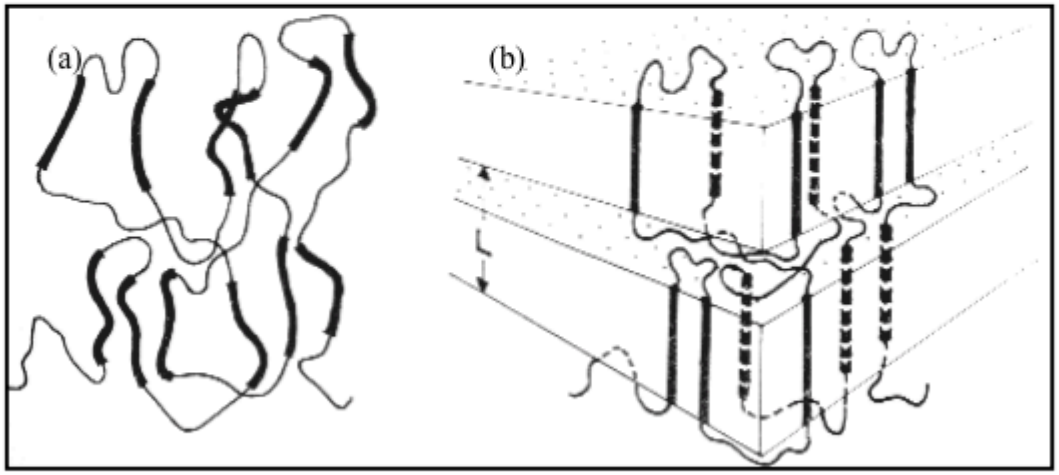

Figure 2.8 "Erstarrungsmodell" (a) chain conformation in the melt state (b) alignment of suitable conformations in to the crystal[36].

Nature of the Chain Fold Surface:

In addition to determination of T◦, the specific nature of the lamellar interface in terms of molecular conformation is of critical importance to the Hoffman analysis. There are several limiting examples, 1) **Regular Adjacent Reentry**, 2) **Switchboard Model** (Non-Adjacent Reentry), 3) **Irregular Adjacent Reentry** (Thickness of interfacial layer is proportional to the temperature).

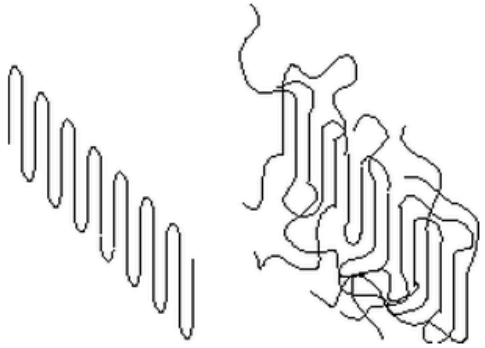

The **synoptic or comprehensive model** involves interconnection between neighboring lamellae through a combination of adjacent and Switchboard models.

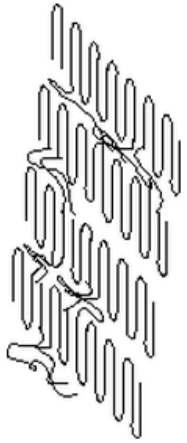

The **interzonal model** involves non-adjacent reentry but considers a region at the interface where the chains are not randomly arranged, effectively creating a three phase system, crystalline, amorphous and interzonal.

http://www.eng.uc.edu/~gbeaucag/Classes/MorphologyofComplexMaterials/Chapter2html/Chapter2.html

Semi-Crystalline Polymer Morphologies and their Hierarchical Morphologies

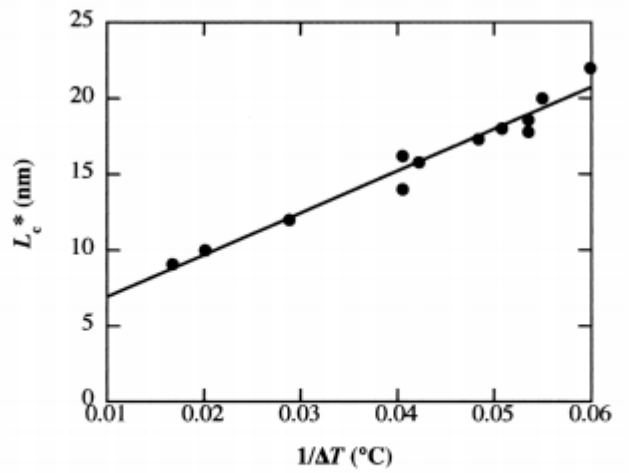

Fig. 6.11. Initial crystal thickness as a function of the reciprocal degree of supercooling (ΔT). Drawn after data of Barham at al. (63).

Semi-Crystalline Polymer Morphologies and their Hierarchical Morphologies

Solution Crystallization

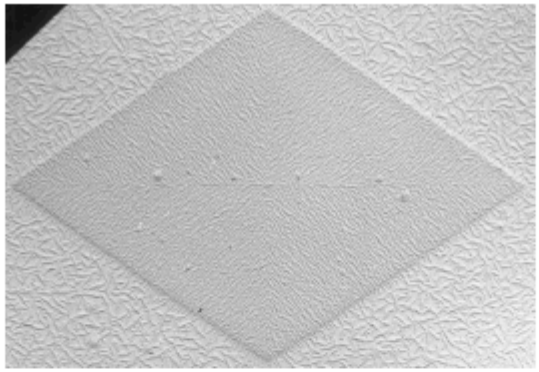

Fig. 6.4. Transmission electron micrograph of a replicate of a single crystal of polyethylene decorated with polyethylene vapour. With permission from Wiley, New York (30).

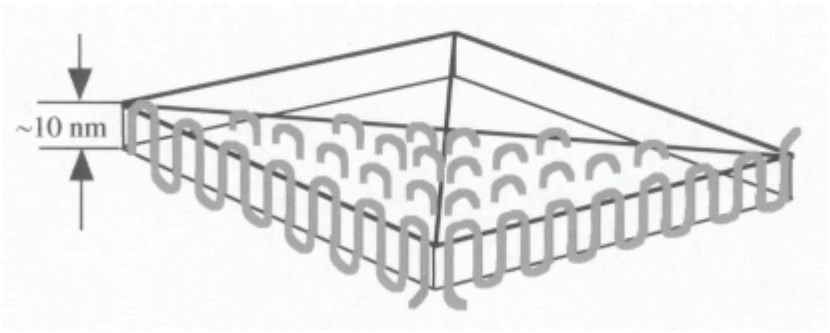

Fig. 6.5. Schematic drawing of single crystal with regular chain folding

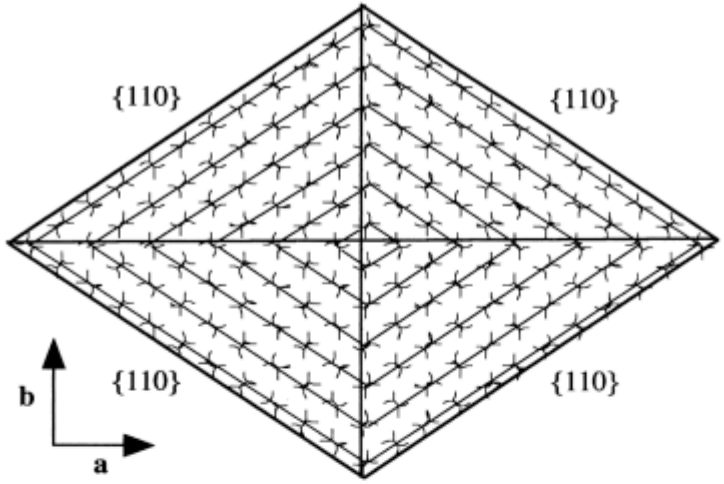

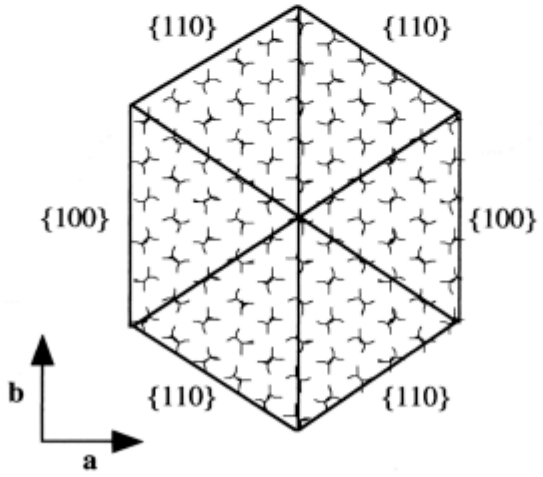

Fig. 6.6. Sectorization of polyethylene single crystals. T{110} sectors whereas the lower also has {100} secKluwer, Doordrecht, the Netherlands (120).

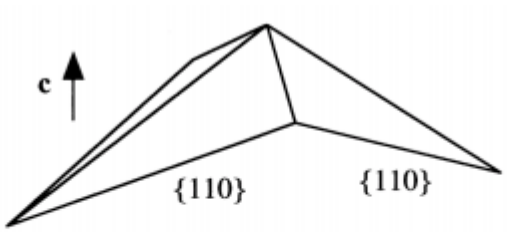

Fig. 6.7. Schematic drawing of tent-shaped polyethylene single crystals with only {110} sectors.

Why do Chains Fold?

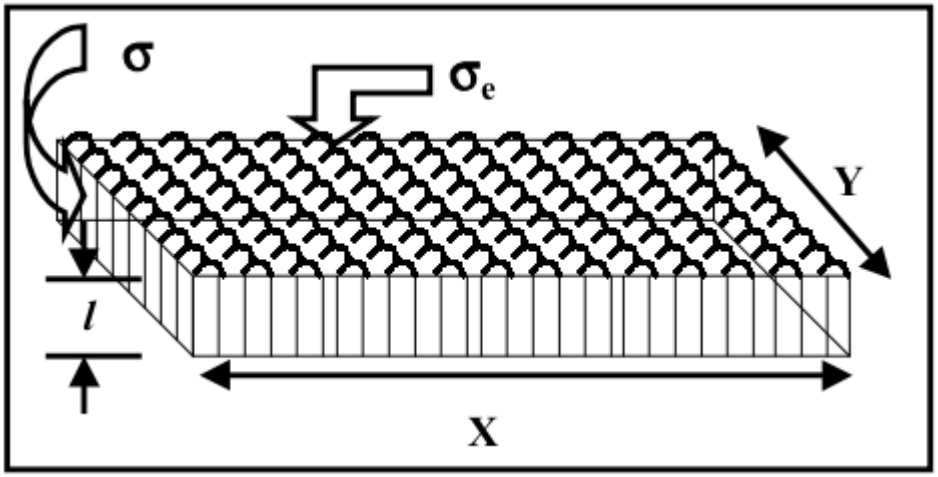

http://scholar.lib.vt.edu/theses/available/etd-051799-162256/unrestricted/polyimide2.pdf

Why do Chains Fold?

$$V\Delta G_{Crystallization} = V\Delta H_{Crystallization} - VT\Delta S_{Crystallization} - S\sigma$$

For an infinite crystal V/S is very large and we can ignore the surface
At the equilibrium melting point ΔG = 0 so:

$$T_{\infty} = \frac{\Delta H_{Crystallization}}{\Delta S_{Crystallization}}$$

substituting in the first equation,

$$V\Delta G_{Crystallization} = V\Delta H_{Crystallization}\left(\frac{T_{\infty} - T}{T_{\infty}}\right) - S\sigma$$

Why do Chains Fold?

$$V\Delta G_{Crystallization} = V\Delta H_{Crystallization}\left(\frac{T_\infty - T}{T_\infty}\right) - S\sigma$$

For a lamellar crystal S is $2R^2$ and V is tR^2

At a pseudo-equilibrium point where the crystal has a finite thickness of t and a depressed melting point, T

$$0 = t\Delta H_{Crystallization}\left(\frac{T_\infty - T}{T_\infty}\right) - 2\sigma$$

$$t = \frac{2\sigma T_\infty}{\Delta H_{Crystallization}\Delta T}$$

Why do Chains Fold?

$$t = \frac{2\sigma T_\infty}{\Delta H_{Crystallization} \Delta T} \quad \text{or} \quad T_m = T_\infty - \frac{2\sigma T_\infty}{t \Delta H_{Crystallization}}$$

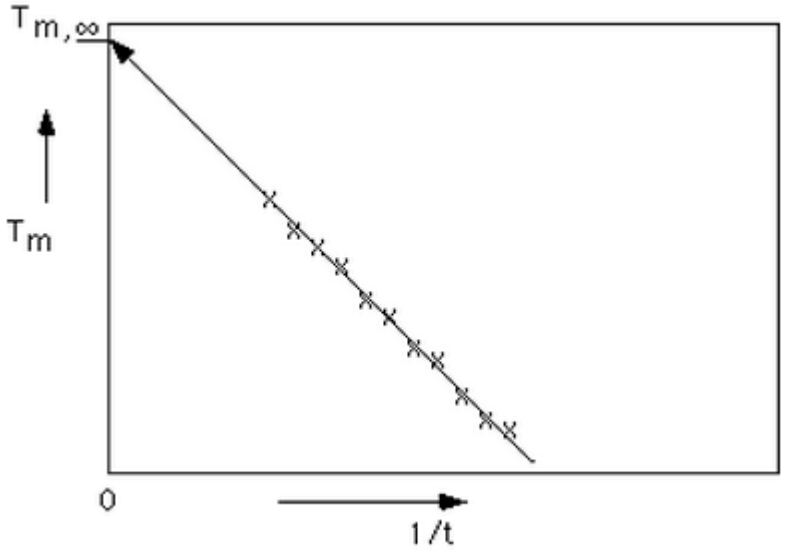

Hoffman-Weeks Plot

Hoffman-Weeks theory is based on the difference between melting, T_m, and crystallization , T_c, temperatures. In the Hoffman-Weeks approach, it is considered that any crystallite formed at temperatures less than $T_\circ$ has some imperfections "locked-in". Generally, the melting temperature is higher than the crystallization temperature, $T_m > T_c$. Hoffman and Weeks defined a stabilization parameter, f', which is zero for crystallites with no imperfections and has a value of 1 for an unstable crystal with all imperfections. For the most stable crystallite $T_m = T_\circ$. For the completely unstable crystallite, $T_m = T_c$. For a typical crystallite, $f'=1/2$. Using a simple weighting law, Hoffman and Weeks wrote a linear expression relating T_m, $T_\circ$ and T_c,

$$T_m = T_\circ(1-f') + f' T_c$$

This linear law implies plots of T_m versus T_c to obtain $T_\circ$ without requiring a measurement of the crystallite thickness. At $T_\circ$, $T_m = T_c = T_\circ$ according to this approach. The Hoffman-Weeks approach and the more direct approach yield very close values for $T_\circ$.

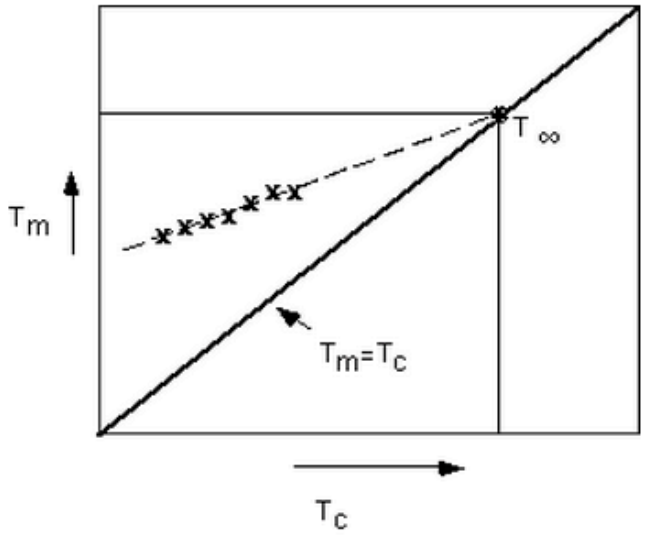

Hoffman-Weeks plot for $T_\circ$.

http://www.eng.uc.edu/~gbeaucag/Classes/MorphologyofComplexMaterials/Chapter2html/Chapter2.html

Semi-Crystalline Polymer Morphologies and their Hierarchical Morphologies

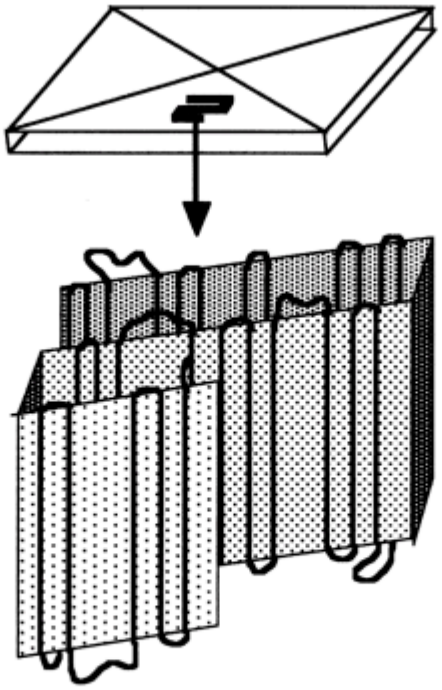

Fig. 6.13. The superfolding model according to Sadler and Keller (84) showing the conformation of a single molecule in a solution-grown single crystal.

Semi-Crystalline Polymer Morphologies and their Hierarchical Morphologies

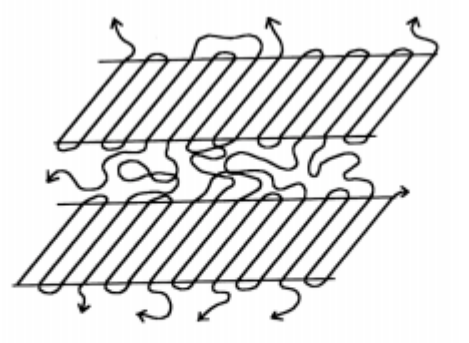

Fig. 6.14. Schematic description how overcrowding of the amorphous phase is avoided by adjacent, regular folding.

Semi-Crystalline Polymer Morphologies and their Hierarchical Morphologies

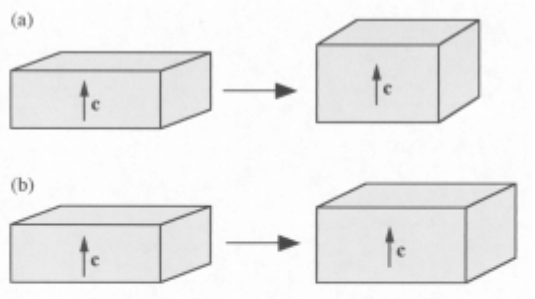

Fig. 6.9. Schematic description of crystal thickening options: (a) Crystal thickening at constant crystal volume. (b) Crystal thickening accompanied by an increase in crystal volume.

Semi-Crystalline Polymer Morphologies and their Hierarchical Morphologies

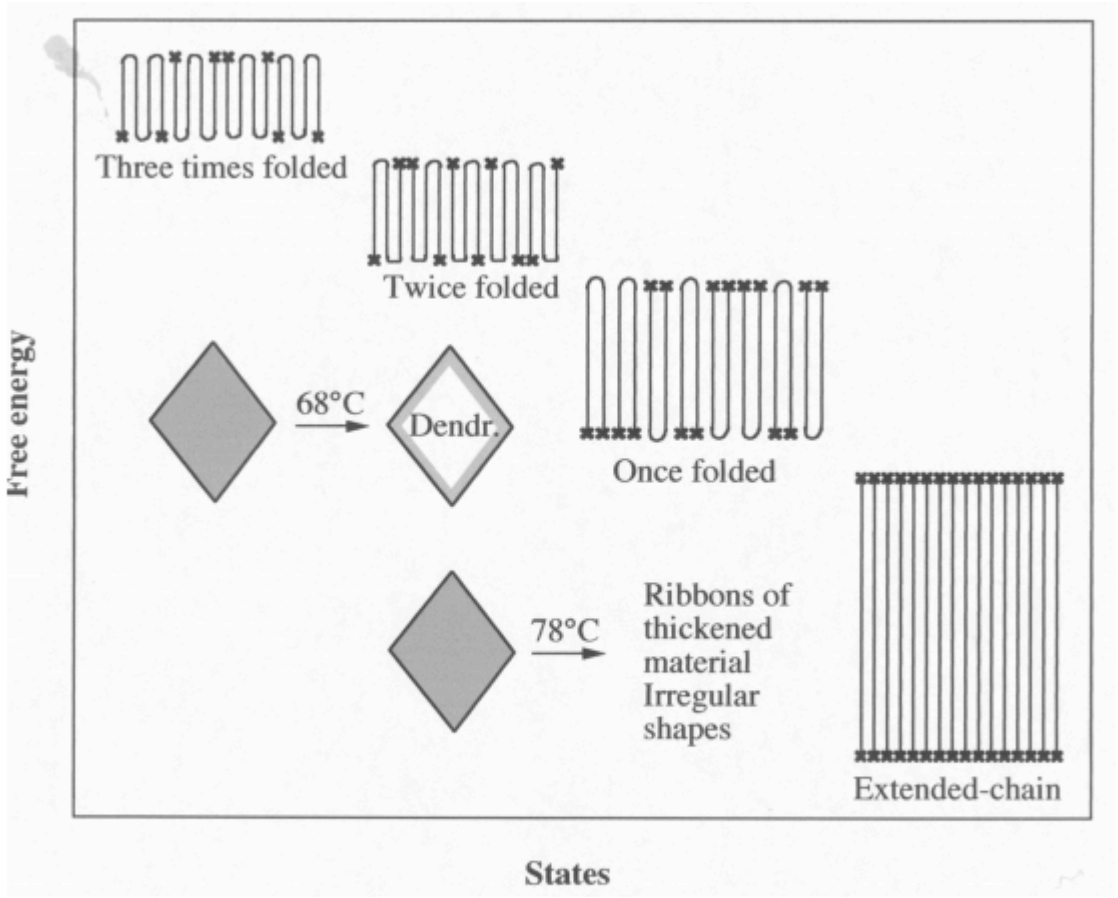

Fig. 6.10. Schematic representation of crystal thickening of $C_{294}H_{590}$. Drawn after findings of Hobbs et al. (51).

Semi-Crystalline Polymer Morphologies and their Hierarchical Morphologies

P J Phillips

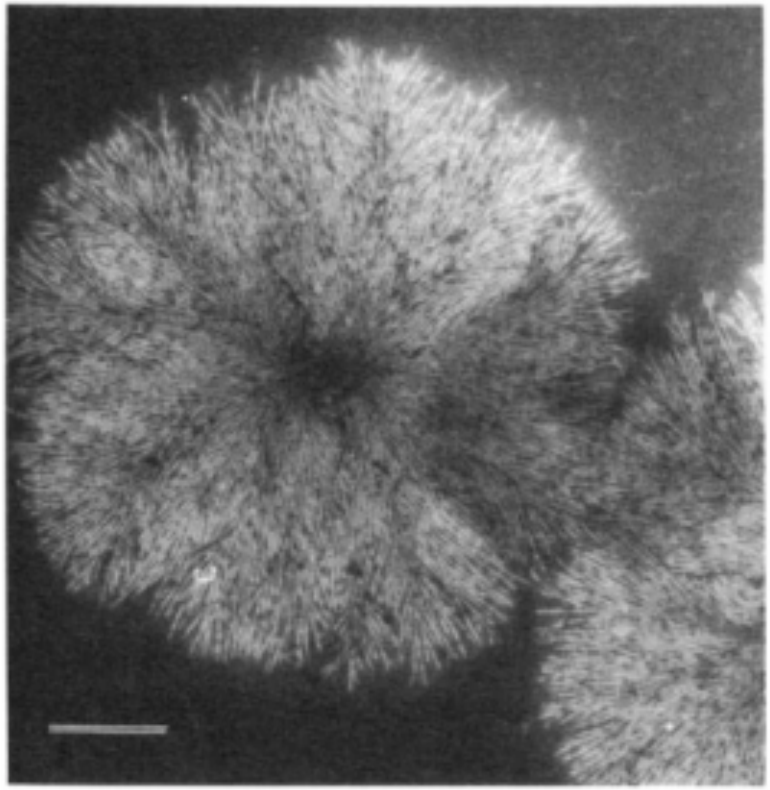

Figure 5. A spherulite growing in a film of *cis*-polyisoprene. The crystal growth has been terminated prior to completion, through reaction of the film with osmium tetraoxide vapour, thereby permitting resolution of the individual lamellar crystals. (Scale bar: 0.5 μm.) First published by Phillips (1983).

Semi-Crystalline Polymer Morphologies and their Hierarchical Morphologies

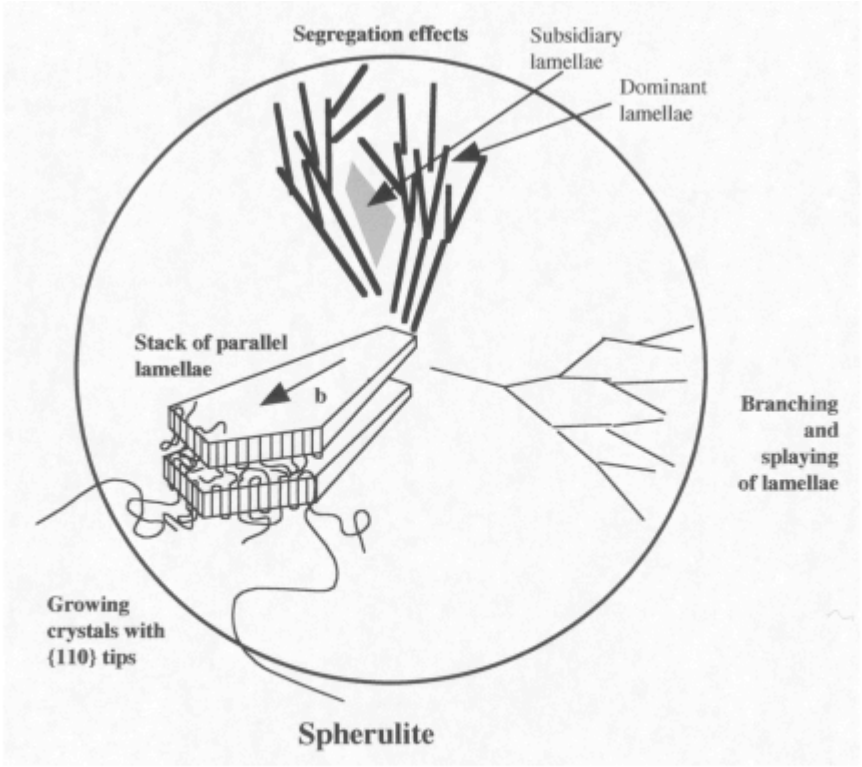

Fig. 6.8. Schematic drawing of the morphological hierarchy of a polyethylene spherulite.

Semi-Crystalline Polymer Morphologies and their Hierarchical Morphologies

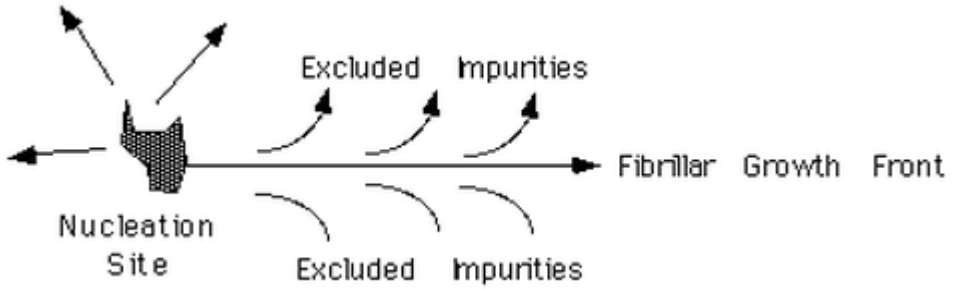

Diffusion of impurities versus growth rate of crystallization front

$J = -D\, dc/dx$ for flux of impurities
G = linear growth rate of crystal

$D/G = \delta$, the Keith-Padden δ-parameter

This determines the coarseness of the spherulite (lateral size)

Semi-Crystalline Polymer Morphologies and their Hierarchical Morphologies

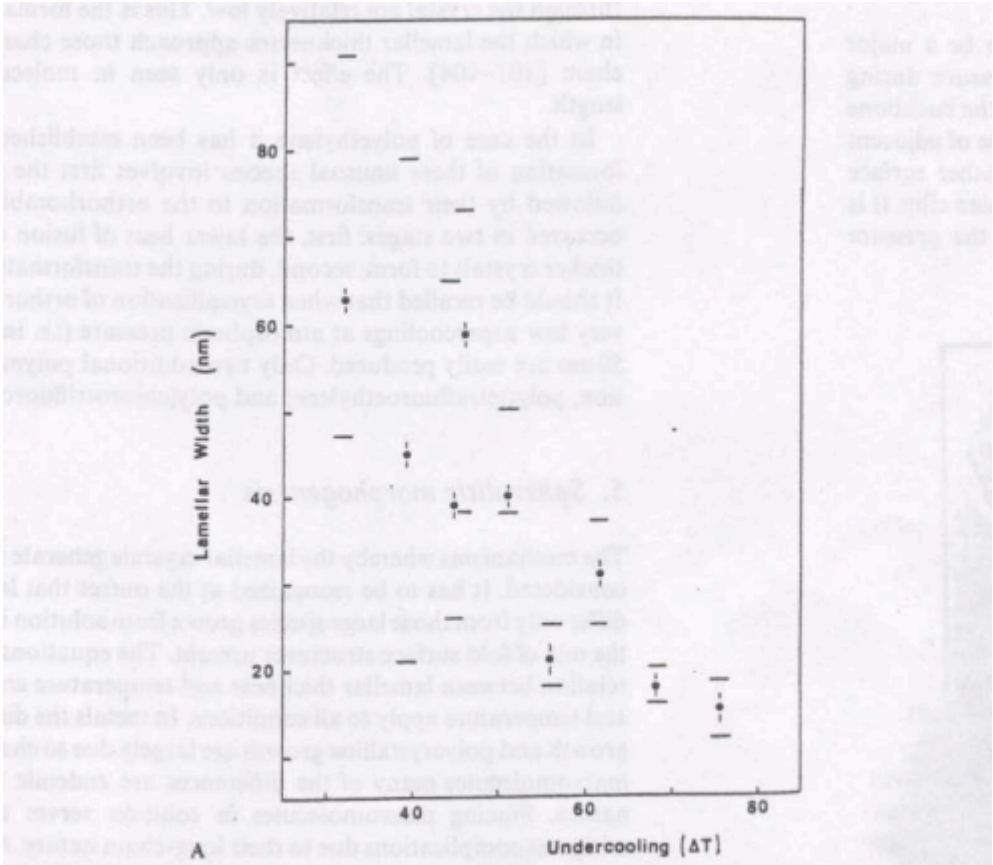

Fig. 28. (A) Distribution of lamellar widths in a fraction of cis-polyisoprene of molecular weight 313 000, and (B) dependence of lamellar width on supercooling at (a) −20°C and (b) −0.6°C (molecular weight 543 000) [108].

Hoffman-Lauritzen Secondary Nucleation Theory

The original L-H theory and its various modifications account for a broad range of behavior observed for crystallization of linear flexible macromolecules. These are[39]:

- it accounts for the variation of initial lamellar thickness (l^*) vs. supercooling (ΔT_c)
- parameters can be found that fit the variation of crystal growth rate 'G' vs. ΔT_c
- provides an explanation for break in temperature dependence of G
- explains the origin of σ and σ_e
- the generation and effect of adjacent events (tight folding) and non-adjacent events (e.g. tie chains, loose folds, cilia)
- Variation of (a) the crystal growth rate 'G' and (b) quantified chain folding (i.e. degree of tight chain folding), with the change in molecular weight
- Recent versions have also incorporated the 'reptation' concept into the theory

http://scholar.lib.vt.edu/theses/available/etd-051799-162256/unrestricted/polyimide2.pdf

Hoffman-Lauritzen Secondary Nucleation Theory

The various facets of polymer crystallization still not addressed completely by the theory are:

- Explanation for primary nucleation and hence bulk crystallization kinetics
- Development of lamellae from a primary nucleus
- Lamellar branching giving rise to spherulites (other factors like screw dislocations provide some explanation)
- Banding in spherulites due to lamellar twisting
- Quantified estimation of the degree of crystallinity

http://scholar.lib.vt.edu/theses/available/etd-051799-162256/unrestricted/polyimide2.pdf

Hoffman-Lauritzen Secondary Nucleation Theory

Add a first stem, then subsequent stems.

First stem and subsequent stems add

$2b_0\sigma l$ and $b_0\sigma l$

To the free energy (cost to make a surface)

http://scholar.lib.vt.edu/theses/available/etd-051799-162256/unrestricted/polyimide2.pdf

Hoffman-Lauritzen Secondary Nucleation Theory

First stem:

Also the change in free energy when going from subcooled melt to the activated stem is:

$$\Delta G_c^* = 2b_0\sigma l + \psi\,[a_0 b_0 l]\,\Delta G_c \qquad \{2.18\}$$

where ΔG_c is the free energy of crystallization/unit volume and 'ψ' is the apportionment factor, i.e. the fraction of free energy available due to the crystallographic attachment at a finite and few number of sites. The possible values of 'ψ' can thus be between 0 and 1.

http://scholar.lib.vt.edu/theses/available/etd-051799-162256/unrestricted/polyimide2.pdf

Hoffman-Lauritzen Secondary Nucleation Theory

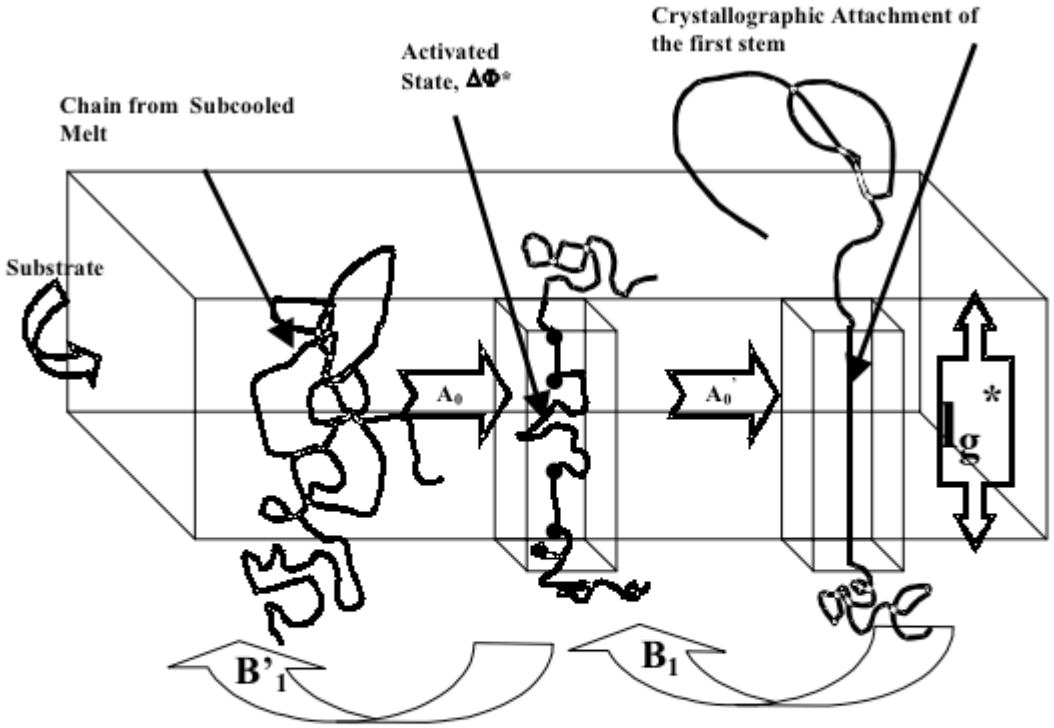

Figure 2.9 Formation of the physically aligned activated complex and its conversion to first crystallographically attached stem. The first step A_0 is the slowest and rate determining step while the step A_0' is fast[39].

http://scholar.lib.vt.edu/theses/available/etd-051799-162256/unrestricted/polyimide2.pdf

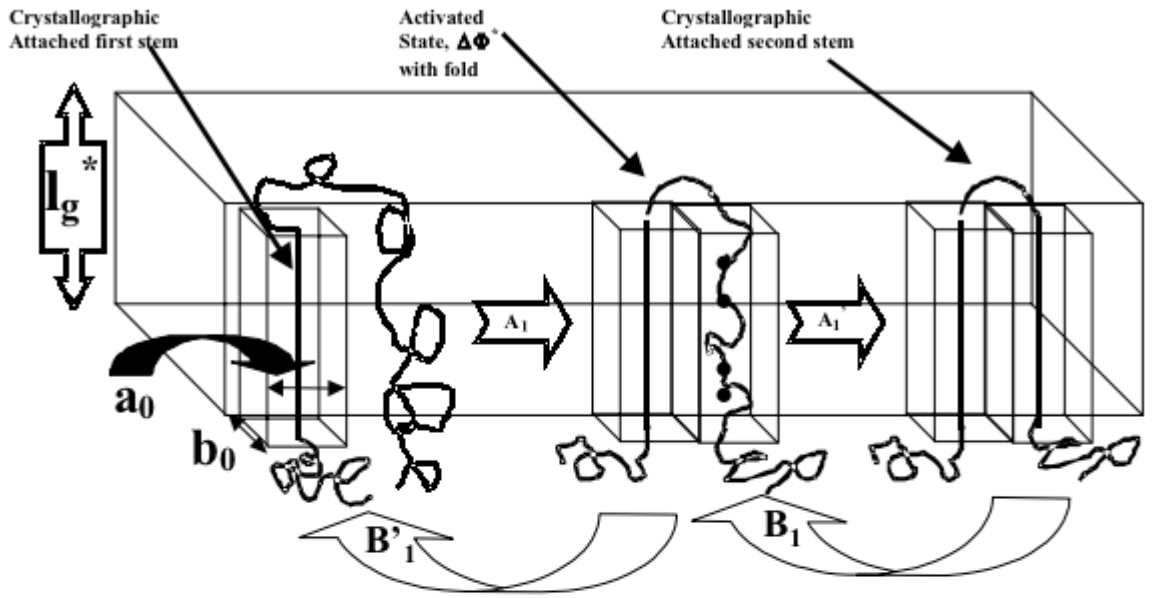

Figure 2.10 Formation of the physically aligned activated complex and its conversion to second crystallographically attached stem. The first step A_0 is the slowest and rate determining step while the step A_0' is fast. The activated state includes a tight fold + the aligned part of the chain[39].

http://scholar.lib.vt.edu/theses/available/etd-051799-162256/unrestricted/polyimide2.pdf

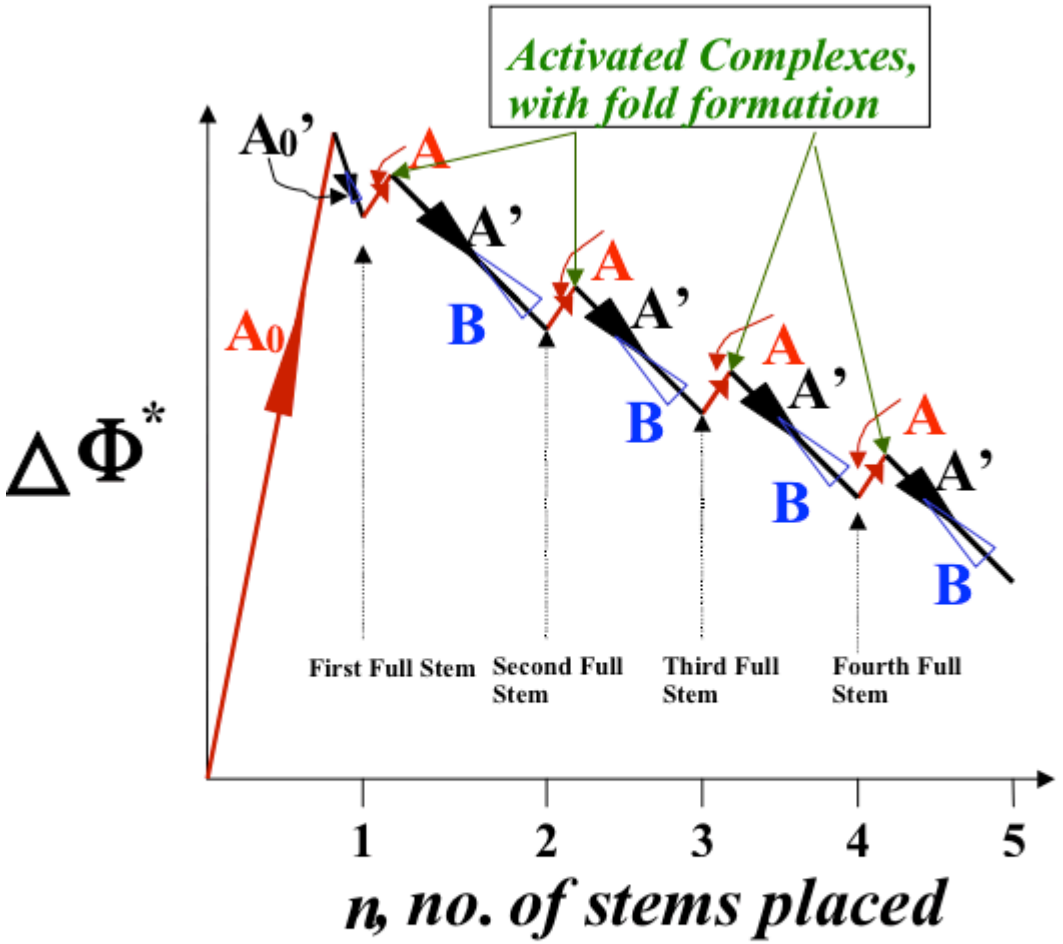

Figure 2.11 Barrier system for the surface nucleation showing both the slow, fast and backward steps possible. A, A_0, B_1 and B are the rate determining slow steps while A_0' and A' are the fast steps[32].

http://scholar.lib.vt.edu/theses/available/etd-051799-162256/unrestricted/polyimide2.pdf

The above-discussed concepts lead us to calculations involving the lateral substrate completion rate, S_T as given by equation (2.35) below. The steady state flux S_T is

$$S_T = \frac{1}{l_u} \int_{2\sigma_e/\Delta G}^{\infty} S(l)dl \qquad \{2.35\}$$

where l_u is the monomer length.

This allows us to calculate the rate of stem deposition 'i', i.e. the surface nucleation rate in terms of stems s^{-1} cm^{-1} by the simple relation[39]

$$i = S_T / L = S_T / n_l a_0 \qquad \{2.36\}$$

where n_l is the number of stems of width a_0 which make up the substrate of length L. The

http://scholar.lib.vt.edu/theses/available/etd-051799-162256/unrestricted/polyimide2.pdf

Hoffman-Lauritzen Secondary Nucleation Theory

second important parameter leading up to the crystal growth rate 'G' is given by the substrate completion rate 'g'. The substrate completion rate is given by

$$g = a_0 (A\text{-}B) \qquad \{2.37\}$$

http://scholar.lib.vt.edu/theses/available/etd-051799-162256/unrestricted/polyimide2.pdf

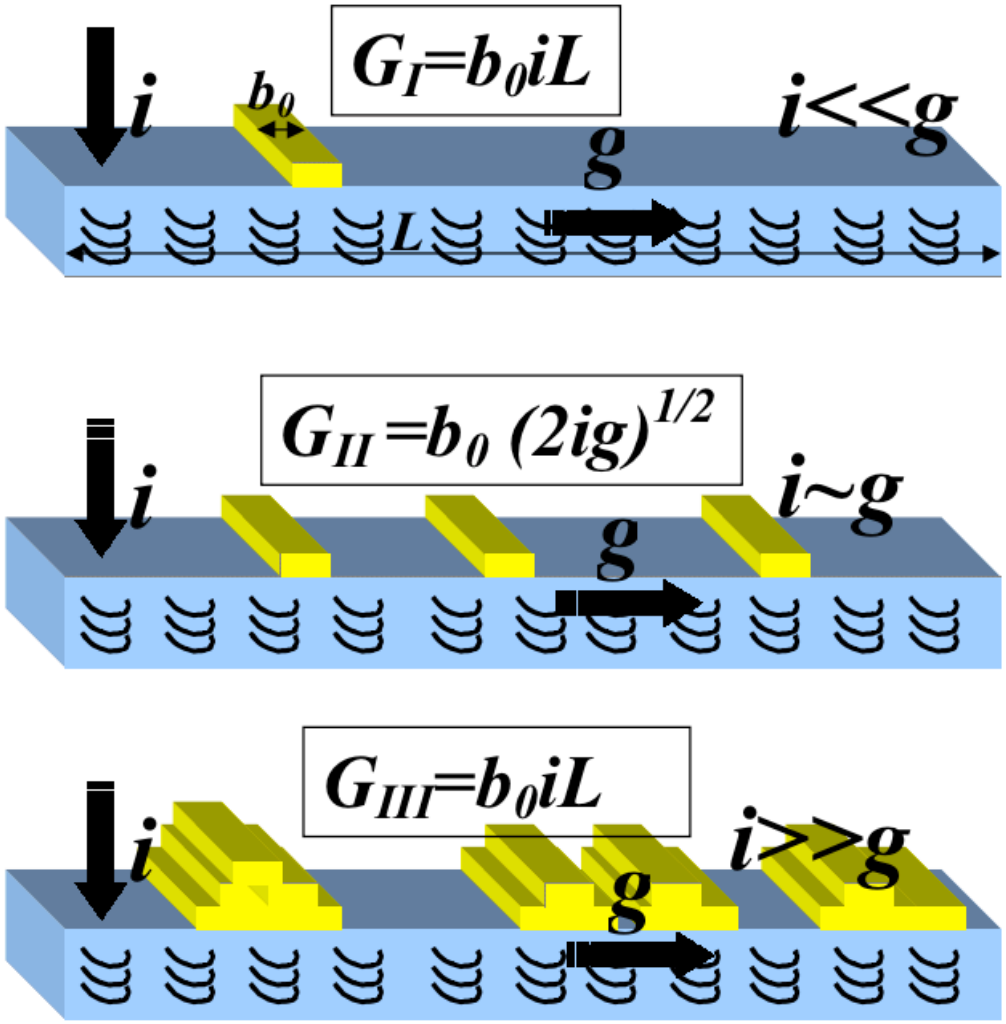

Figure 2.13 Scheme illustrating the rates of stem deposition during three different regimes of crystallization. 'i' represents the rate of stem nucleation whereas 'g' represents the rate of substrate completion.

http://scholar.lib.vt.edu/theses/available/etd-051799-162256/unrestricted/polyimide2.pdf

Hoffman-Lauritzen Secondary Nucleation Theory

$$i = \frac{N_0 \beta}{n_l a_0 l_u}\left[\frac{kT}{2b_0\sigma} - \frac{kT}{2b_0\sigma + \Delta G_f}\right]\exp\left[\frac{-4b_0\sigma_e\sigma}{\Delta G_f kT}\right] \qquad \{2.38\}$$

$$g = a_0\beta\left[1 - \exp\left(\frac{a_0 b_0 \delta l \Delta G_f}{kT}\right)\right]\exp\left[\frac{-2a_0 b_0 \sigma_e}{kT}\right]$$

$$\beta = J\exp\left[\frac{-U^*}{R(T-T_\infty)}\right] \qquad J = \frac{\kappa}{n}\left(\frac{kT}{h}\right)$$

http://scholar.lib.vt.edu/theses/available/etd-051799-162256/unrestricted/polyimide2.pdf

Hoffman-Lauritzen Secondary Nucleation Theory

$$G_I = G_{0I} \exp\left(-U^*/R\,(T-T_\infty)\right) \exp\left(-K_{gI}/T\Delta T_c\right)$$

$$G_{II} = G_{0II} \exp\left(-U^*/R\,(T-T_\infty)\right) \exp\left(-K_{gII}/T\Delta T_c\right)$$

$$G_{III} = G_{0III} \exp\left(-U^*/R\,(T-T_\infty)\right) \exp\left(-K_{gIII}/T\Delta T_c\right)$$

$$G_{0i} = \frac{N_0 b_0 J}{l_u}\left[\frac{kT}{b_0\sigma} - \frac{kT}{2b_0\sigma + a_0 b_0 \Delta G_f}\right]$$

$$K_{gI} = K_{gII} = 2K_{gIII} = \frac{4\sigma\sigma_e T_m}{k\Delta H_f}$$

http://scholar.lib.vt.edu/theses/available/etd-051799-162256/unrestricted/polyimide2.pdf

Hoffman-Lauritzen Secondary Nucleation Theory

The value of the nucleation constants K_{gI}, K_{gIII}, K_{gII} and G_{0i} can thus be determined by plotting the spherulitic growth rate data in the form $LnG + U^*/R\,(T-T_\infty)$ vs. $1/\,T\Delta T_c$. These types of plots are usually referred to as L-H plots and Figure 2.13 illustrates the typical plots for polymers showing these transitions. The first exponential term in equation (2.40), $\exp(-U^*/R\,(T-T_\infty))$ accounts for the chain transport effects to the interface while the second term $\exp(-K_{gi}/T\Delta T_c)$, accounts for the secondary nucleation effects. The widely utilized values for U^* and T_∞ are 1500 cal/mol and T_g-30K for a large number of polymers[39,43]. L-H plots have also been widely utilized to obtain values for $\sigma\sigma_e$ if the values of T_m°, ΔH_f and b_0 are known[40,58,59,60], or otherwise sometimes to obtain T_m° [54,61,62].

http://scholar.lib.vt.edu/theses/available/etd-051799-162256/unrestricted/polyimide2.pdf

Hoffman-Lauritzen Secondary Nucleation Theory

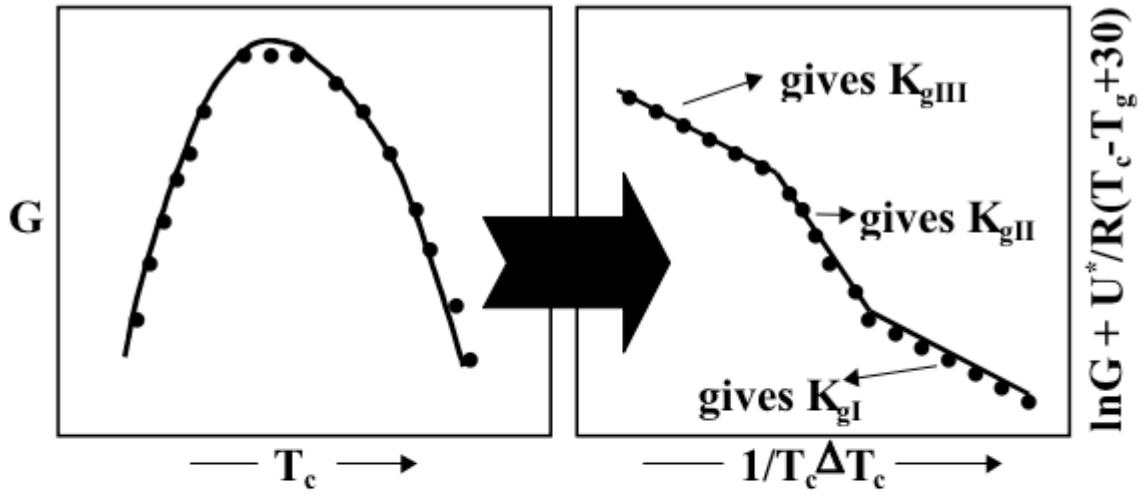

Figure 2.14 A schematic illustrating the conversion of growth rate data to a L-H plot showing the three regime transitions[38]. The values of regime constants are calculated by the slope in various regimes and are used to give the product of surface energy terms $\sigma\sigma_e$. All three regimes or even a single regime transition may not be experimentally observed for many polymers.

http://scholar.lib.vt.edu/theses/available/etd-051799-162256/unrestricted/polyimide2.pdf

Primary Nucleation

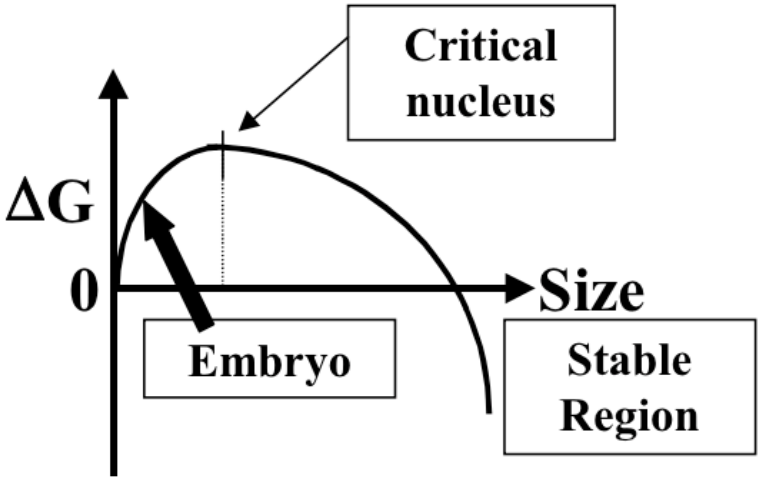

Figure 2.15 Schematic illustrating the variation of free energy with nucleus size. The initial free energy barrier needs to be crossed for the nucleus to become stable[5].

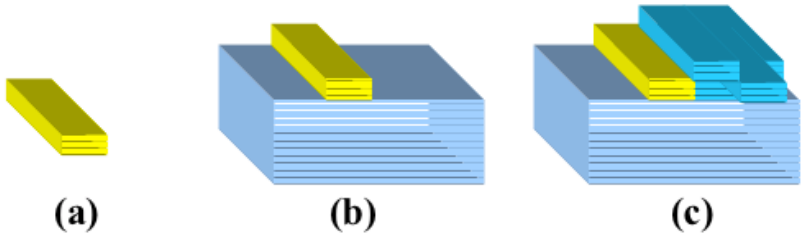

Figure 2.16 Types of Crystal Nuclei (a) Primary nucleus (b) Secondary Nucleus (c) Tertiary Nucleus

http://scholar.lib.vt.edu/theses/available/etd-051799-162256/unrestricted/polyimide2.pdf

Primary Nucleation

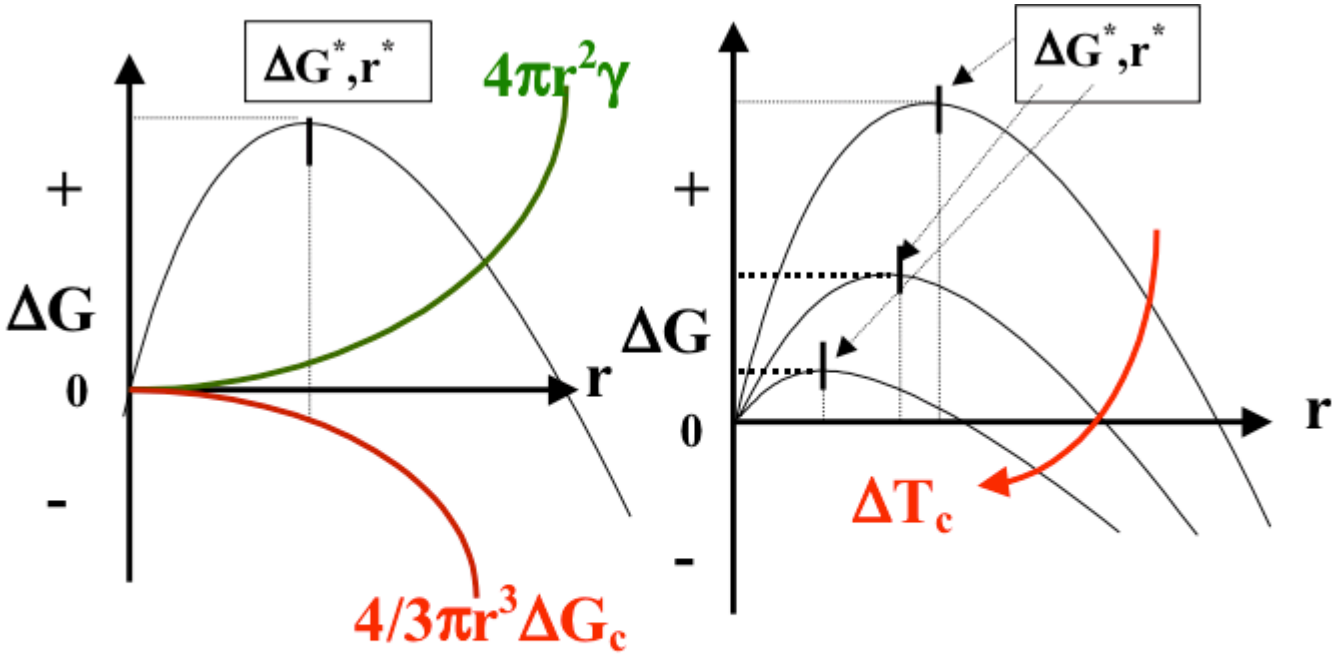

Figure 2.17 Variation of total free energy with size depends upon two opposing factors, the gain being due to increased surface area while the loss due to free energy of crystallization. Also, the critical size for stable nuclei formation as well as the critical free energy barrier decrease with increasing undercooling[2,38].

http://scholar.lib.vt.edu/theses/available/etd-051799-162256/unrestricted/polyimide2.pdf

Spherulites

Figure 2.18 Tie chains in polyethylene spherulites crystallized in presence of n-parafin, $C_{32}H_{66}$, and then extracted with xylene at room temperature. (Keith and Padden[70] et al.)

http://scholar.lib.vt.edu/theses/available/etd-051799-162256/unrestricted/polyimide2.pdf

Primary Nucleation

http://scholar.lib.vt.edu/theses/available/etd-051799-162256/unrestricted/polyimide2.pdf

Semi-Crystalline Polymer Morphologies and their Hierarchical Morphologies

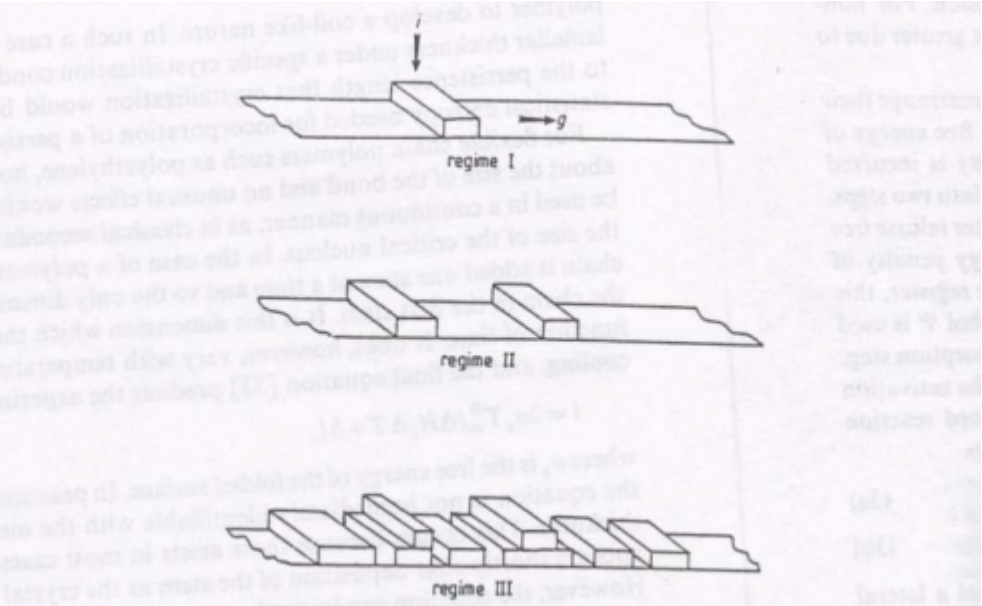

Fig. 21. Schematic diagram of secondary nucleation profiles in the three regimes of polymer crystallization (first published in [3]).

Semi-Crystalline Polymer Morphologies and their Hierarchical Morphologies

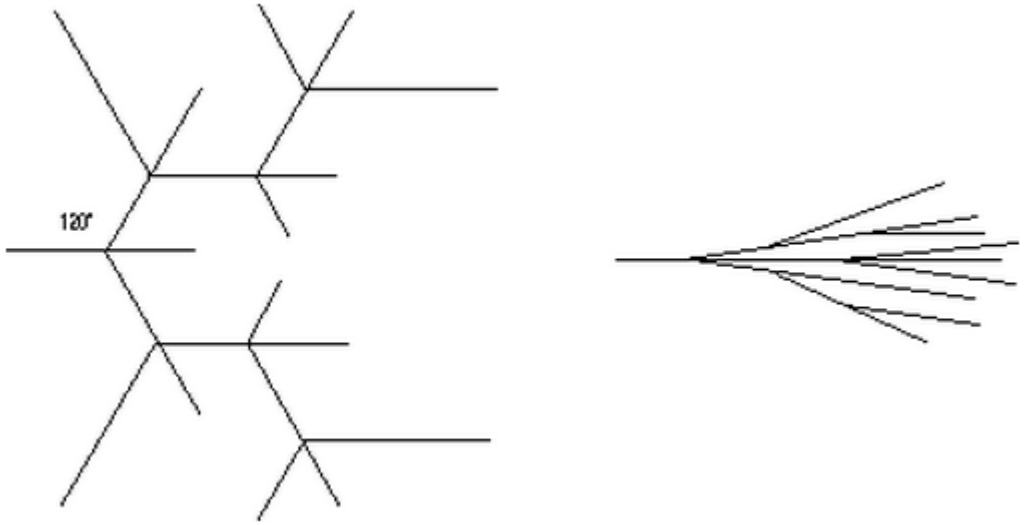

ttp://www.eng.uc.edu/~gbeaucag/Classes/MorphologyofComplexMaterials/Chapter2html/Chapter2.html

Semi-Crystalline Polymer Morphologies and their Hierarchical Morphologies

Non Crystallographic Branching

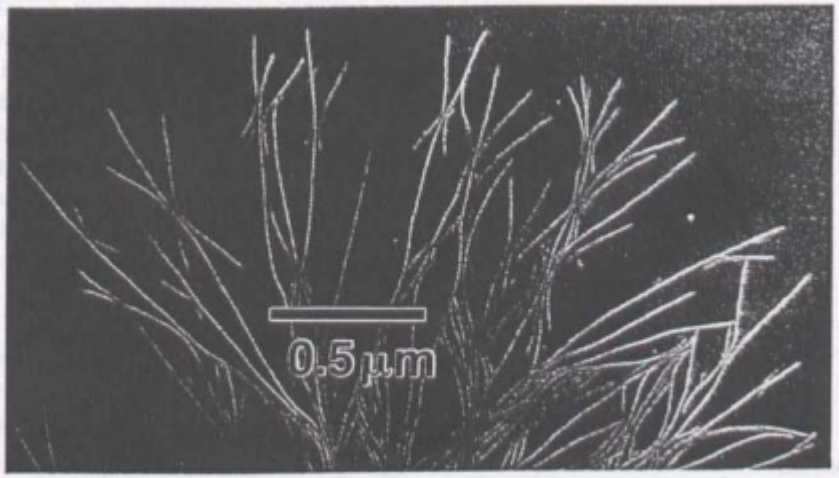

Fig. 29. Non-crystallographic branching in cis-polyisoprene crystallized at −15°C.

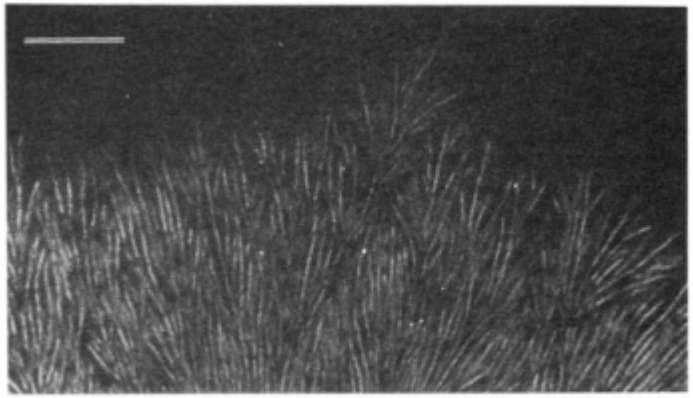

Figure 21. Leading lamellae protruding ahead of the growth front in a beta-spherulite of *cis*-polyisoprene. Due to extensive crystallographic branching, the protuberances are smaller than in spherulites of alpha-crystals of the same polymer. Scale bar 0.2 μm. (Sorenson and Phillips, unpublished data).

Figure 19. Transmission electron micrograph of a shadowed carbon replica of permanganically etched linear polyethylene showing ridged crystals. The specimen ($M_w = 37\,000$, $M_n = 29\,000$) had been crystallised at 130 °C for 7.5 days followed by 30 min at 125 °C prior to a cold-water quench. (Bassett and Hodge, unpublished work. Photograph supplied by D C Bassett.)

Semi-Crystalline Polymer Morphologies and their Hierarchical Morphologies

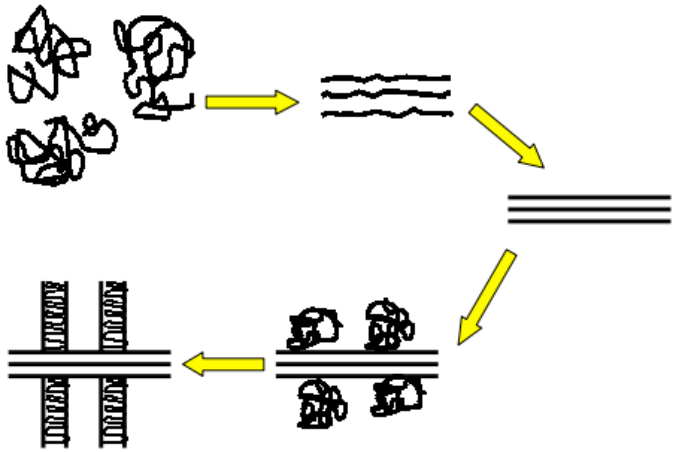

Figure 2.3 Schematic representation of orientation induced crystallization. The first three drawings illustrate the orientation and crystallization of random coils while the last two drawings show the growth of folded chain kebabs around the central shish[10].

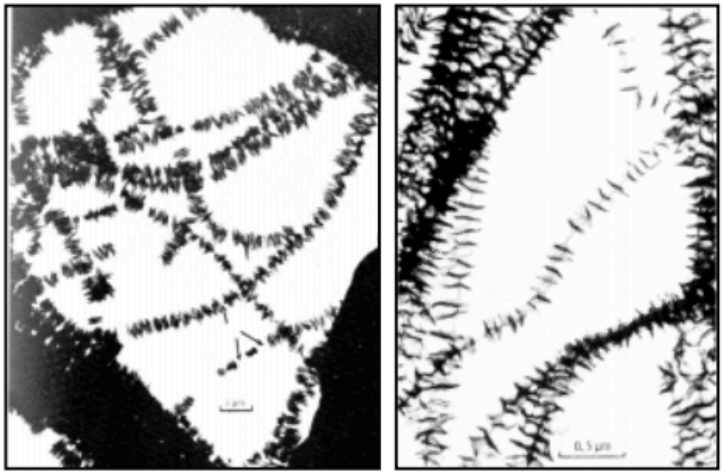

Figure 2.4 (a) Shish kebab morphology of polyethylene from solution (from Pennings, 1967[3]. (b) Shish kebabs of cellulose formed by recrystallizing cellulose II onto microfibrils of high molecular weight[3].

Semi-Crystalline Polymer Morphologies and their Hierarchical Morphologies

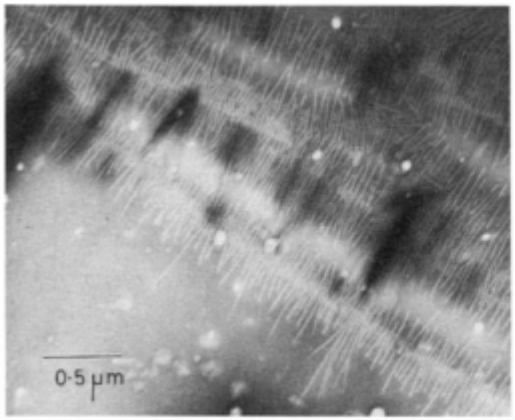

Figure 20. Row-nucleated growth (shish-kebabs) in *cis*-polyisoprene (Edwards and Phillips, unpublished data).

Spherulitic Growth Rate

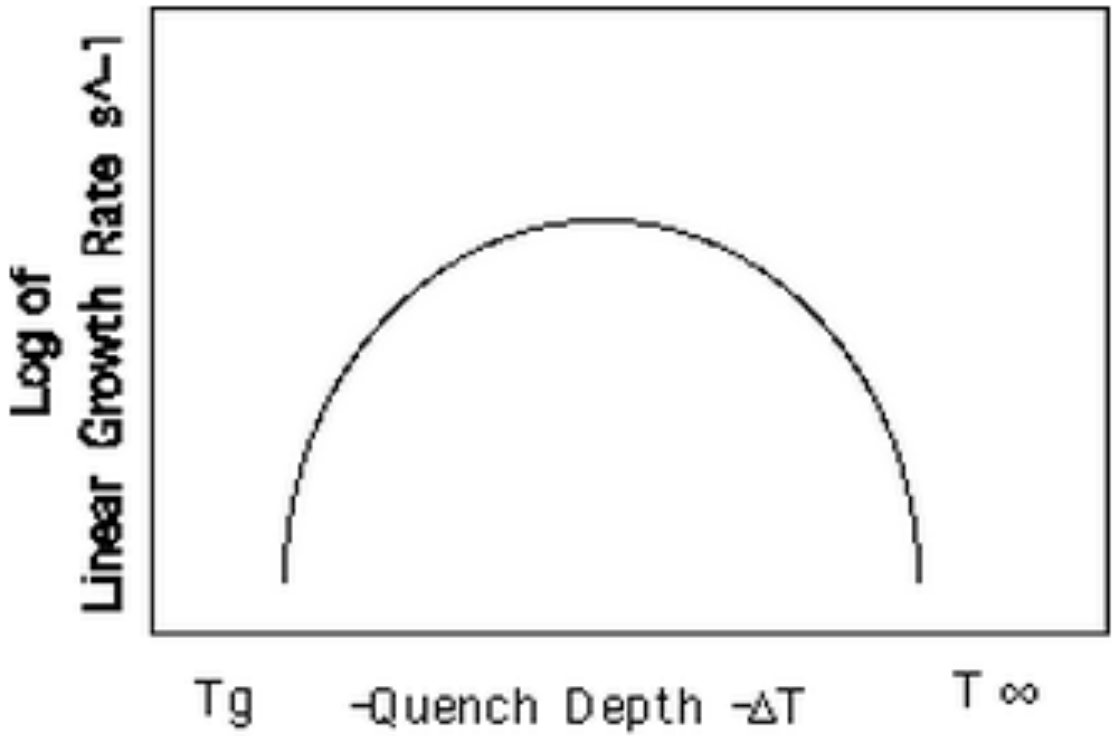

Avrami Equation

Poisson[81] in 1837, which states that for raindrops falling randomly, the probability of a point being passed over by exactly F wavefronts is given by

$$P(F) = \frac{e^{-\overline{F}}\overline{F}^{F}}{F!} \qquad \{2.48\}$$

where $\overline{F}$ is the average number of such wavefronts passing through a point. Thus considering these wavefronts as spherulites in bulk crystallization, the probability of any point not being run over by a spherulite is given by value of P(F) at F=0. Thus

$$P(0) = e^{-\overline{F}} \qquad \{2.49\}$$

P(0) also represents the points which are still amorphous and not been run over by the spherulites and thus is equal to amorphous fraction 1-θ, where θ is the amount of fraction crystallized.

$$\begin{aligned} 1-\theta &= P(0) = e^{-\overline{F}} \\ \Rightarrow \ln\frac{1}{1-\theta} &= \overline{F} \\ \Rightarrow \theta &= 1-\exp(-\overline{F}) \end{aligned} \qquad \{2.50\}$$

Now the problem reduces to obtaining the form of the function $\overline{F}$ for different types of geometries that may be involved. The time dependency of the crystalline fraction in the above analysis enters due to time dependency of the function $\overline{F}$, the average number of

http://scholar.lib.vt.edu/theses/available/etd-051799-162256/unrestricted/polyimide2.pdf

Avrami Equation

wavefronts passing in time 't'. For some particular cases, this function can be calculated to give the following relations[5,82]:

(a) 2-dimensional case of growing discs starting at the same time

$$\overline{F} = \pi G^2 N t^2 \qquad \{2.51\}$$

where G is the growth rate of growing discs, N is the average number of such discs/area and t is the elapsed time.

(b) 2-dimensional case of growing discs forming at a rate $\dot{N}$

$$\overline{F} = \frac{\pi}{3} G^2 \dot{N} t^3 \qquad \{2.52\}$$

(c) 3-dimensional case of growing spheres starting at the same time

$$\overline{F} = \frac{4}{3} \pi G^3 N t^3 \qquad \{2.53\}$$

(d) 3-dimensional case of growing spheres forming at a rate $\dot{N}$

$$\overline{F} = \frac{\pi}{3} G^3 \dot{N} t^4 \qquad \{2.54\}$$

In general then, the form of the equation is of the type

$$\boxed{\theta = 1 - \exp(-Kt^n)} \qquad \{2.55\}$$

which is the famous Avrami equation and the 'K' & 'n' are the two Avrami parameters

http://scholar.lib.vt.edu/theses/available/etd-051799-162256/unrestricted/polyimide2.pdf

Avrami Equation

Table 2.2. Avrami exponents for various types of crystal growth geometry's[82].

Avrami Exponent	Crystal Geometry	Nucleation Type	Rate Determination
0.5	Rod	Athermal	Diffusion
1	Rod	Athermal	Nucleation
1.5	Rod	Thermal	Diffusion
2	Rod	Thermal	Nucleation
1	Disc	Athermal	Diffusion
2	Disc	Athermal	Nucleation
2	Disc	Thermal	Diffusion
3	Disc	Thermal	Nucleation
1.5	Sphere	Athermal	Diffusion
2.5	Sphere	Thermal	Diffusion
3	Sphere	Athermal	Nucleation
4	Sphere	Thermal	Nucleation

http://scholar.lib.vt.edu/theses/available/etd-051799-162256/unrestricted/polyimide2.pdf

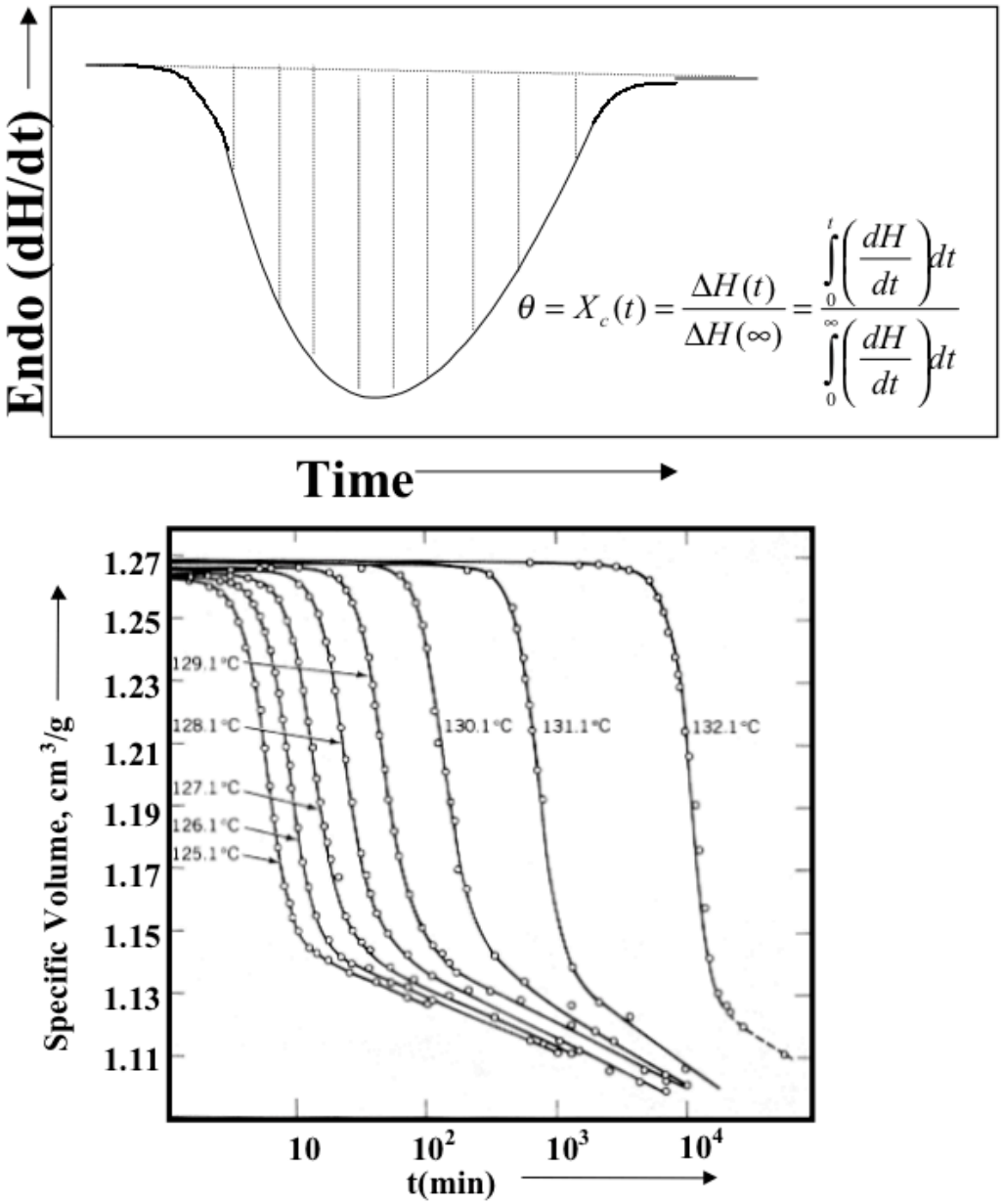

Figure 2.19 Utilization of isothermal crystallization data by either DSC or by volume[30] measurements can give the degree of transformation, which can subsequently be utilized for Avrami analysis.

http://scholar.lib.vt.edu/theses/available/etd-051799-162256/unrestricted/polyimide2.pdf

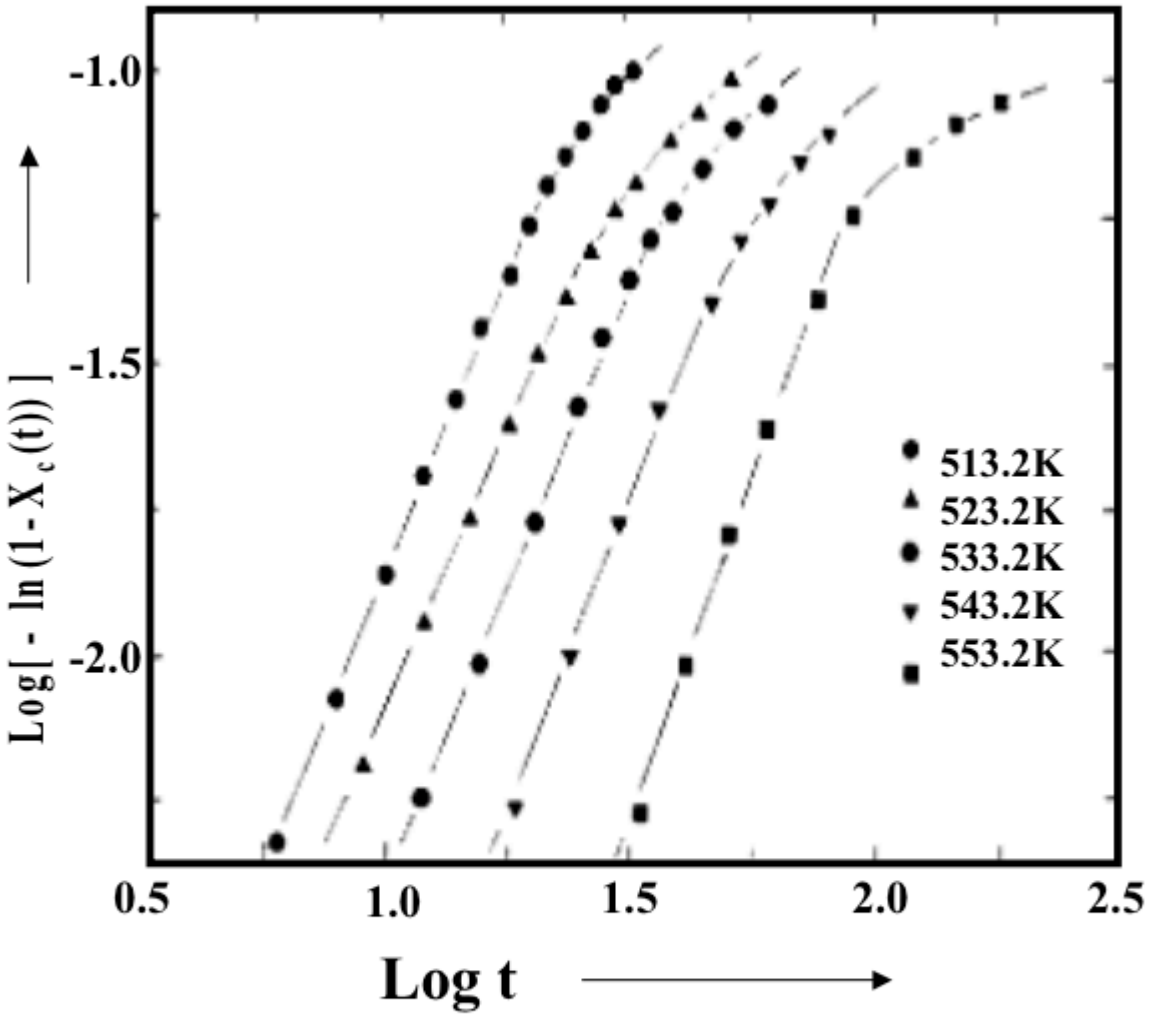

Figure 2.20 The characteristic Avrami plots obtained by isothermal crystallization experiments for a polyimide[84]. The initial slope of the curves gives the Avrami constant 'n', which is related to the crystal shape and nucleation type.

http://scholar.lib.vt.edu/theses/available/etd-051799-162256/unrestricted/polyimide2.pdf

Avrami Equation

(a) The Avrami equation rigorously applies only to problems where the volume does not change. This is never the case with crystallization in polymers.

(b) It assumes constancy in the shape of growing disc/rod/sphere

(c) Constant radial growth is assumed ($G \sim t^{-1/2}$ has also been considered)

(d) The analysis does not account for the presence of an induction time

(e) The nucleation mode is assumed to be unique i.e. thermal or athermal but not both

(f) Complete crystallinity of the sample

(g) Random distribution of nuclei

(h) Constant value of radial density in the growing structures which is assumed in the derivation does not usually occur experimentally

(i) Holds well for primary crystallization only

(j) Does not account for absence of overlap between growing crystallization fronts

It is thus not surprising that non-integer values of n are often obtained. As shown in Table 2, it is not difficult to assign the experimentally obtained value of n by selecting an appropriate geometry. This kind of attribution of the exponent 'n', without independent microscopical evidence is one of the major pitfalls of most studies in the literature utilizing this analysis. *Independent microscopical evidence is critical before assignment of 'n' to a particular geometry can be justified.*

http://scholar.lib.vt.edu/theses/available/etd-051799-162256/unrestricted/polyimide2.pdf